Ashesi University

DESIGN AND FABRICATION OF A SOLAR-POWERED ELECTRIC STOVE FOR RURAL AND URBAN COMMUNITIES OF GHANA

Capstone

B.Sc. Mechanical Engineering

David Attuah

(ID: 98672019)

May 2019

ASHESI UNIVERSITY

Design and fabrication of a solar-powered electric stove for rural and urban communities of Ghana

APPLIED

CAPSTONE PROJECT

Capstone Project submitted to the Department of Engineering, Ashesi University in partial fulfilment of the requirements for the award of Bachelor of Science degree in Mechanical Engineering.

David Attuah

May 2019

Declaration

I hereby declare that this capstone is the result of my own original work and that no part of it has been presented for another degree in this university or elsewhere.

Candidate's Name: ……

Candidate's Signature: ……...

Date: …….

I hereby declare that preparation and presentation of this capstone were supervised in accordance with the guidelines on supervision of capstone laid down by Ashesi University.

Supervisor's Name: ……

Supervisor's Signature: ……

Date: ……

Acknowledgements

I am most grateful to God Almighty for His grace and goodness throughout my studies, especially during the execution of this project.

Furthermore, I would like to thank Dr Danyuo Yiporo for his support and guidance throughout the project. He was indeed an active supervisor.

Appreciation is also extended to Nicholas Tali and Joseph Timpabi for their technical advice and support.

Table of Contents

List of Figures

List of Tables

Abstract

This report presents the optimisation of a ceramic-matrix composite (anthill sand and cement), reinforced with treated coir fibres for applications in the construction of a low cost-solar powered cooking stove to solve the current trends in the depletion of forest spaces in Ghana due to excessive destruction as a result of using firewood for cooking by a higher percentage of rural communities. The reinforced coir fibres reduce undesirable traits in ceramics including, low fracture toughness and low flexural strength. Sample characterisation involved; fibre modification, tensile tests of fibres, three-point bend tests on the composites, water absorption tests on the composite materials, hardness tests, and compressive tests. A prototype was developed and tested for thermal performance and analysis before the first prospective model of the stove was fabricated.

Dedication

I dedicate this work to the engineering department of Ashesi University.

Chapter One

Introduction

1.1 Background Studies

The source of energy for cooking plays a vital role in the overall cost of domestic cooking in our homes. The most common sources of energy for cooking include biofuels (biogas, firewood and others.), liquefied petroleum gas and electricity. Depending on the economic context in question, these sources vary with their levels of usage. These energy sources can generally be classified as either renewable or non-renewable.

World Bank statistics for Africa show that 94% of the entire African rural population as well as 73% of the urban population, , rely on firewood as a primary source of energy for domestic cooking [1]. Firewood happens to be the primary source of energy for cooking in rural households in Ghana [2]. Statistics confirm that firewood consumption has reported figures between 1.62-2.77kg/capita/day in the country [2].

This trend of firewood consumption has led to a more significant depletion of the forestry in Ghana, with a variety of plant species being used for firewood [2]. 41.3% of households in Ghana use firewood as a primary cooking energy source [3]. Methods of reducing deforestation include the use of solar energy as an alternative source of energy for cooking. The use of solar energy in daily applications is still in its infant years as solar sources provided only 10% of worldwide energy [4]. Nevertheless, solar energy is already in use for domestic applications. Solar energy has already been implemented in some parts of the world, including Ghana where solar dryers are used to solve the problems and drawbacks that open sun-drying methods present. Open sun-drying causes 20-30% losses in crop produce [5].

1.2 Problem Definition

The closest, convenient and cleaner source of energy for cooking is Liquefied Petroleum Gas (LPG). This source of fuel is quite expensive, interim, and not readily available in some regions of the country. Hence, the demand and justification for firewood and charcoal usage become rampant [5]. These forms of fuel have been long existed in the country and hence form a significant component of the cooking culture in typical rural areas and some urban homes.

The forestry in Nigeria (used as a case study) declines at an annual rate of 3.5% due to different activities [5] The article also documents the rising demand for forest products for a variety of reasons, as well as wood collection for domestic fuel, which contributes as a causative factor for deforestation in the African context [5]. Deforestation then gives rise to several environmental problems including climate change. The main problem with deforestation lies in the fact that depleted trees are lost over time to bare land. With the evolution of technology in this modern era, a befitting solution to this problem may be through the introduction of electric stoves to save the environment as well as individuals from the dangers of using wood fuels. Nonetheless, the current energy generation and distribution state of the country makes this solution almost impossible. First, electricity usage is expensive due to the cost of generation and distribution. Hence many households barely can afford electricity for cooking. Also, electricity distribution does not have nationwide coverage yet. Thus many rural areas have no access to electricity.

Also, the current electric stoves come in large and heavy packages and have it installed by electrical wiring, which is impossible in most rural communities, given the knowledge that several homes in our rural communities do not have access to on-grid electricity. In the case for homes that do have access to electricity, electric cooking would tend to be an expensive

cooking option, although cleaner and safer, especially if such a home is in a rural or underdeveloped community in Ghana.

For these reasons, homes in deprived communities continue to use wood from trees as fuel for their domestic purposes, which in turn leads to or contributes in some way to the problem of desertification and deforestation of our natural vegetative cover as a country and the world, generally. In addition to this global issue, the use of firewood as a fuel source produces much smoke which is usually uncontrolled and left to blow into the atmosphere, contributing to air pollution and in effect, global warming.

1.3 Objectives of the Project

This project seeks to innovatively design and fabricate an electric stove which would utilise solar energy to address critical drawbacks of the current stoves while providing its target market with cost flexibility, safety and efficient cooking system.

The following specific objectives would be addressed in this project:

- To conduct proper materials selection with Cambridge Engineering Selector (CES Edupack 213) for the design and construction of a modern solar stove.
- To construct a stove that makes use of solar energy converted into heating for cooking.
- To mechanically simulate the thermal and electrical performance of the solar cooker with SolidWorks.
- To ensure selected materials can provide excellent insulation properties.
- To analyse the mechanical, electrical and thermal properties of the solar cooker.

1.4 Justification/Motivation of the Project

About the above-discussed problem space, members of households in rural communities settle for firewood as a primary source of fuel due to its availability and a relatively cheaper option when compared with other alternatives. This research introduces a method of utilising solar energy as a renewable source for cooking. Figures show that the average annual household expenditure in rural communities in Ghana stands at Ghc 1,514 annually, with 43.2% spent on foodstuff, 8.7% on clothing and the remainder on a combination of housing, electricity (if access is available) and gas [6], which shows that little money is made available for cooking. This solution would address the central issue of deforestation while taking into consideration, the rural household income of the country to ensure that the solution presented can still be affordable for its target market. To achieve this, materials for creating this new development would be sourced locally to construct a low-cost stove.

1.5 Expected Outcome

It is expected that upon completion of this project, the following expectations would be met;

- Fully developed encasement serving the purpose of housing an electrical system developed as a converter of solar energy into an efficient source of heat for cooking.
- Correctly formulated methodology of the entire project, for referral and future reference.
    - High fracture toughness.
    - High strength.
    - Low coefficient of thermal conductivity.
    - High thermal shock resistance.
    - Light in weight.

Chapter Two
Literature Review

2.1 Background Statistics

Access to modern cooking facilities and energy has been identified since 2014, as a fundamental issue affecting multitudes in developing countries. This concern has been a critical factor influencing the inclusiveness of 'Renewable Energy' as the seventh Sustainable Development Goals adopted by the United Nations in 2015 [8]. The issue of lack of access to sustainable energy sources cannot be overemphasised. However, data gathered in 2013 by the International Energy Agency (IEA) suggest that 1.26 billion people do not have access to electricity worldwide [8][9]. The IEA statistics also show that 2.64 billion people are confined to using traditional cooking methods, daily [8][9]. Aside the problem of deforestation, the use of the traditional cooking methods and a heavy reliance on energy sources like biomass and charcoal create other problems including health problems in the respiratory system as well as air pollution. Four million people die annually from the pollution that results from the use of traditional cooking methods [8]. Further statistical evidence shows that areas affected by this phenomenon are concentrated in Asia and Africa, totally accounting up to 84% of the world's population [8]. The use of renewable energy sources for cooking presents various benefits including their benefits to the environment and reliability in developing countries, reduction in operational cost of non-renewable energy sources, and repetitive buying of resources for cooking [10].

The use of solar power for cooking stands as a brilliant alternative to the current traditional methods employed in Africa. Due to the positioning of the continent concerning the sun, 85% of the continent receives at least 2,000 kWh/ (m^2 year) [10], which puts Africa in a

right place to utilize the abundant solar power needed, not only for cooking purposes but also, to provide solutions across energy issues on the continent. However, solar power is underutilised for various reasons including high upfront costs, dependence on climatic factors, lack of financial support and lack of engineering skills and technical know-how [10].

Countries in Africa have been scrutinised concerning the amount of energy used and the costs at which they are run. Morocco was used as a case study to estimate the unit price of solar photovoltaic energy. Research shows that aside the amount of solar radiation available to any region under study, indirect factors affect the feasibility of running solar powered systems in Africa [11]. Due to the financial and economic standing of Africa currently, most homes cannot meet the cost demanded by solar systems due to factors such as inflation rates, discount rates, mortgage fees and installation cost [11]. These make it challenging to run a solar-powered plant in most African countries.

2.1. Solar Heating Technologies

Heating through resistance wires would be implemented in this project. The designed cooking device would work based on the principle of resistance heating. In the general design of electric cooking devices, two different methods of heating are applicable; namely heating by induction and by resistance [12]. Under heating by induction, high frequencies are supplied to induction coils, producing a strong magnetic field. This magnetic field, in turn, produces eddy currents and magnetic hysteresis, from which heat is supplied to the utensils [12]. The alternative to this is resistance heating, which makes use of a wire that opposes current flow and causes heat to be generated in the process.

Induction cookers are generally more efficient than resistance heaters [11]. However, the project would make use of resistance heaters because, for a pilot project, the benefits of

low cost and easier maintenance are preferred [11]. In addition to that, the project attempts to optimise around the use of one solar panel, and due to the enormous current demands of induction cookers, a lot of solar panels would be necessary if induction is to be implemented.

On a wide scale, stoves which utilise convection or heat generation through fuel sources use almost similar materials in internal construction since it is quite an essential and underlying property of stoves to produce a heat source for cooking. For this reason, most cooking stoves require materials with high insulation-properties to form encasements. The final product should be safe and not cause burns or any form of heat-related hazards for that matter. Other design-based criteria are used to inform the material selection and overall design of the final product.

The temperature ranges, as well as the corrosive environment which stoves are used, require that materials used should possess the necessary properties to ensure performance is kept at the required level [12]. For safety reasons and to ensure that the stove does not fail, suitable materials are selected to ensure that quality is maintained throughout the lifespan of the stove.

Different considerations are usually given during the design process, including decision making based on different properties and functions of the stove. Some of these properties and functions include the strength of the material used in making all parts of the stove, durability, insulation properties, thermal conductivity, the mass flow of heat through the system, heat transfer and safety hazards associated with the design of the stove components.

2.2 Stove Cooktops

Stoves are made from a variety of materials, including ceramics and metals, usually modified in their mechanical and chemical properties [12]. The main interface of modern stoves, the cooktops also vary in design and material selection, each informed by the different

characteristics intended to be possessed by the stove. Wood burning stoves have been constructed with materials such as sheet iron, cast iron, aluminium, limestone and different ceramics. Within the African context, several rural communities are populated with households which patronise stoves or cooking spaces made up of refractory materials [14]. These materials are usually relied upon because of their durability and their ability to withstand high temperatures that would be generated during cooking [13]. Refractory materials are known to withstand temperatures of about 538°C, which makes them suitable for use in cooking applications [13]. These refractory materials also have excellent insulative properties which allow them to serve as good options for constructing stoves. Other materials, including metals like stainless steel and other alloys, are also used. However, given the criteria of material selection based on economic factors such as cost of manufacture, ease of manufacture, availability of resources/ materials as well as design-based selection criteria including weight, thermal insulative properties and durability, materials for constructive the stove are limited to the scope of ceramics.

2.3 Ceramics

Ceramics, because of their properties serve as preferred materials for applications involving heat or generally high temperatures; some of which include cooking applications. Ceramic materials also possess other desirable characteristics including low density, chemical inertness, high hardness and high strength. [15] Ceramic products also hold acclaim to attractive finishes and pleasing aesthetics [16]. Albeit these properties, ceramic materials, due to their nanocrystalline nature and microscopic structure, happen to be brittle due to recorded values of low fracture toughness. This property restricts the application of ceramics in many endeavours, and for this reason, there is a high level of research into strengthening techniques for a variety of ceramic products [15]. In different efforts to improve the abilities of ceramics,

the use of the knowledge of composite materials is currently being applied in the area of ceramics. Reinforced structural ceramics are stronger than conventional ceramics. Ceramic composites are tested and proven to have modified and superior abilities than they occur in their united states [17]. These composites show improvement in the ceramic's properties about high-temperatures and fracture toughness [17]. Ceramic composites also have higher thermal shock capacities as compared to plain, unmodified ceramics [18].

Different materials are used as reinforcement in ceramic matrix composites. Based on the scope of the project and the objective of using locally acquired materials, the focus would be on the use of fibres as reinforcements for the ceramic mix selected.

2.4 Modification of Ceramics

As discussed, modifications are made to the structure of the ceramic materials in order to enhance its abilities. These mechanisms, after research was done by Rice and Shetty, can be classified into two parts; strengthening and toughening mechanisms. [18]. Under these mechanisms, a few techniques which apply to the project were identified.

2.4.1 Strengthening Mechanisms

2.4.1.1 Load Transfer

Load transfer requires Young's elastic modulus of the fibre used to be a minimum of twice as higher than Young's elastic modulus of the matrix. Therefore, the ratio $\frac{E_{fiber}}{E_{matrix}} \geq 2$ [18]. With load transfer, load is transferred from the matrix interface to strengthened whiskers or fibers to reduce load impact on the matrix [18].

2.4.1.2 Matrix Prestressing

This mechanism is used on the premise of the knowledge that stresses build up in the ceramic matrix if the thermal expansion coefficient of the fibres is higher than the thermal expansion coefficient of the matrix [18]

From the knowledge gathered in these two mechanisms, design factors are set such that the required ratio of elastic moduli between fibre and matrix is above 2 and also that fibres with the right thermal expansion coefficient are used, given the ceramic matrix composition used.

2.4.2 Toughening Mechanisms

2.4.2.1 Crack Deflection

Crack deflection is a phenomenon which occurs in ceramic matrices during thermal expansion. Cracks are dependent on thermal expansion. If the thermal expansion coefficient of the fibres used is higher than the thermal expansion coefficient of the matrix, the fibres experience radial tension [18]. For this reason, any cracks that build up in the matrix would deflect around the fibres. However, if the thermal expansion coefficient of the fibre used is lesser than that of the matrix, then cracks are attracted towards the matrix instead. Faber and Evans developed crack deflection toughening and describe how effective the use of objects such as rods and fibres are in deflecting cracks by increasing fracture surface area.

2.4.2.2 Whisker/ Fiber Pullout

Fibres with high transverse fracture toughness are used so that failure or fracture occurs only along with the interface between the fibres and the matrix. Under this mechanism, the composite is toughened because extra work is required by any force to pull out the whiskers. For this mechanism to be effective, knowledge of the shear resistance between the matrix and

the fibre is essential, as it helps to determine the paths and arrangement of fibres within the matrix.

2.4.2.3 Wake Toughening

This mechanism is similar to whisker pullouts. The only differing feature, in this case, is that whiskers bridge along the crack faces when there is a fracture. These bridging whiskers restrict the crack opening displacement and reduce further elongation of cracks.

2.5 Fiber Reinforcements

The composite material to be constructed would use a selected fibre as a reinforcement. To suit the low-cost criteria for the project, fibres that are relatively cheap and readily available in Ghana would be considered.

2.6 Coconut Fiber

Coconut fibre happens to be abundant in tropical regions in the world, such as Ghana. Coconut fibres are extracted from the outer shell of a coconut [19]. Also known as coir fibre, they exist in two forms; brown fibre and white fibre [19]. Brown fibres are thicker and stronger, drawn from matured coconuts, while white fibres tend to be weaker and from immature fibres [20]. Statistics report that about 500,000 tons of coir fibre are produced in a year worldwide [20]. Of this number, coconut fibres are produced commercially in three forms; bristle, mattress and decorticated fibres, with the main distinction between the three, are their lengths [19]. Bristles are longer while mattresses are short in length. Decorticated coconut fibres include a mix of long and short fibres. Coconut fibres possess advantageous properties including resistance to fungi, functional sound-proofing abilities, toughness, durability, flame retardance and good resilience. [19]. Their physical and mechanical properties are however challenging to specify and conclude upon, as variations are evident in their properties for similar samples tested [19]. An example is given in one piece of literature where the magnitudes of tensile

strength for different fibres vary although the diameters of the same fibres were approximately the same [19]. Coconut fibres contain cellulose, lignin and hemi-cellulose. The composition of fibre differs by type, and the properties of the coconut fibres are affected by the composition of the fibres. [20]. These properties further affect the properties of composite materials that are made from coconut fibres.

Within the field of composite manufacturing, coconut fibres are used widely in different matrices including cement paste, cement-sand mortar, and concrete. Coir fibres are reported to improve properties of their matrices such as compressive strengths, modulus of rupture and shear strength [21]. In one study conducted by Baruah and Talukdar, the compressive strength of coir fibre reinforced concrete sample increased by 13.7%, its modulus of rapture was improved by 28% and its shear strength was improved by 32.7% [21].

Coconut fibres are therefore used in different civil engineering applications including the manufacturing of plaster, roofing materials, slabs and wall panelling systems. They are also used in applications outside civil engineering which include bulletproof vests, car parts and motorcycle helmets [21]. Its versatility makes it a fibre that is of enormous consideration. To the project at hand, given the claim that coconut fibres are also capable of withstanding the strain of about four to six times more than other fibres [21].

2.7 Scope of Work

The project introduced the problems of deforestation and desertification in Ghana which results from burning and cutting down of trees for firewood and other domestic cooking purposes. Chapter One presented the problem definition, motivation for — the project and justification of the project. The expected outcomes of the project were also presented. In

Chapter Two, research into related topics and similar works were outlined as a basis upon which the project work would be built.

Chapter Three of this paper outlines the experimental methods to be carried out in testing — the materials to be used for the project. The materials would be tested in samples and the specimen yielding the desired results would be selected for use in the prototype model built. Chapter Four presents the results of the experiments with several discussions about trends and figures generated after testing. The discussions would reveal the outcomes of the project.

Chapter Five concludes the project based on the results obtained and additionally presents recommendations for future works while highlighting the limitations encountered in carrying out the project.

Chapter Three

Materials and Methods

3.1 Materials and Methods

3.1.1 Materials

The materials used in designing the stove were selected based on functional properties. It is expected that the composite for the stove should possess high strength, low fracture toughness, low coefficient of thermal conductivity, high insulation, and lightweight. The ceramics to be studied for the composite's matrix include; laterite and sand which were sorted from Ashesi environment. Limestone and fired clay, and cement were purchased from a seller in Berekuso. Fibres for testing include sisal and coconut fibres. The Cambridge Engineering Selector (CES 2013) software (Granta Design, Cambridge, United Kingdom) allowed for a wide range of general properties of ceramics to be sorted for the composite matrix and fibres for the reinforcements.

The requirements of the final product were informed by the; strength, hardness, high fracture toughness, good thermal insulation, light in weight, and low cost.

The available materials were compared against each other and ranked in quality of their properties to inform the decisions of the selections made. The selection criteria were applied to both classes of materials for reinforcements and matrix for the composite to be constructed.

3.4 Experimental Procedures

3.4.1 Fiber Removal and Pulping

Coir fibres were obtained from the Western region, Akosuno, in a local community farm, Ghana. Fibres were peeled off manually from the coconut shell in a process known as fibre retting. The coir fibres were then washed with 2% detergent and rinsed with pipe water. The coir fibres were then soaked in solutions of sodium hydroxide (NaOH) at different concentrations (Fig. 3.1) to determine the optimal concentration for the pulping process. Fibres were removed at intervals of six hours after being soaked in the NaOH solutions. For twenty-four hours of pulping, this process, therefore, requires that there are sixteen samples under testing.

Table 3.1*:Variables of Test Samples for Comparison*

Sample Group	**Duration (hours)**	**The concentration of NaOH (wt.%)**			
Group 1	6	5	6	7	8
Group 2	12	5	6	7	8
Group 3	18	5	6	7	8
Group 4	24	5	6	7	8

***Figure 3.1**: The fibres after hours in NaOH Solution: 5 wt%, six wt%, seven wt% and eight wt% NaOH solution.*

***Figure 3.2**: Fibers During the Drying Process.*

3.4.2 Mortar Ratio

Under this test, the ratio of cement, laterite and sand to be mixed in the matrix was varied repeatedly until desirable results were found. From the reviewed literature, the best mortar mix ratios for any ceramic structure to have excellent strength characteristics ranges between mix ratios of 1:2 to 1:6 [26], where the figures represent the ratios quantity or parts of the binder used to the number of parts of the aggregate used. Mortar ratios between 1:4 and 1:6 reportedly produce structures with good compressive strengths, durability and water absorption [26] — the combination of both forms the matrix base for the composite mix. The optimum mix was determined from sample characterisation for strength and weight.

3.4.3 Tensile Test

The tensile test was performed on the coir fibres using the MTS Exceed extensometer/ tensile testing machine (Model E43, MTS, Eden Prairie, Minneapolis, United States). For the accuracy of results, the fibres were placed within the grip of cardboard slits that was placed within the jaws of the testing machine (Fig. 3.3). Fibres were subjected to load at a loading rate of (5mm/s). The test was performed in triplicates, and average values were reported. Stress-strain curves were then obtained subsequently. From the derived graph, different properties including; the yield strength, Young's modulus, and tensile strength of the fibre were obtained. Moreover, other values derived were the ultimate tensile strength and elongations at selected loads under tension.

Following a fibre pullout test, the debonding shear strength (τ_d) was also determined using the formula; [23]:

$$\tau_d = \frac{F_d}{2\pi r l_e} \tag{3.1}$$

Where F_d is the debonding force, l_e is the embedded length, and r is the radius of the fibre. The test samples were arranged in a manner that exposes some of the fibres at one end of the testing sample, while some fibre length is embedded into the matrix. Both ends of the sample were then clipped and pulled apart. The force at which the fibres were pulled out of the matrix were as well recorded.

The critical fibre length was then determined from the formula; [23]

$$l_c = \frac{\sigma d}{2\tau} \tag{3.2}$$

where $\sigma \; and \; \tau$ are the ultimate tensile strength and shear strength, respectively.

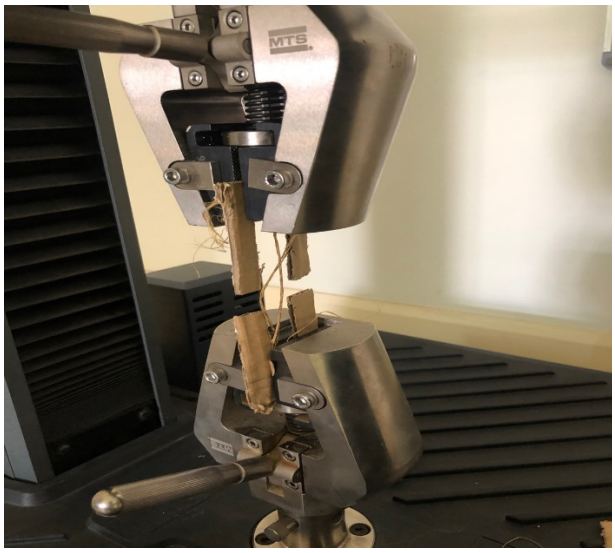

***Figure 3.3**: Illustration of fibres under test using the MTS Testing Machine.*

3.4.4 Effect of fibres in the matrix

This test varies the amount of fibre used in the composite material and the effect of variations on the properties of the composite material. The number of fibres used was varied in terms of the ratio of parts used to mould/fabricate the materials. Percentage compositions (wt% of fibres) were; 10%, 20% and 30 The nomenclature is provided in the table below.

***Table 3.2**: Compositions of Samples*

Composite Sample Name	Compositions
C1	Cement (1 part) + Laterite (2 parts) + Coir (10 wt%)
C2	Cement (1 part) + Laterite (2 parts) + Coir (20 wt%)
C3	Cement (1 part) + Laterite (2 parts) + Coir (30 wt%)
C4	Cement (1 part) + Laterite (3 parts) + Coir (10 wt%)
C5	Cement (1 part) + Laterite (3 parts) + Coir (20 wt%)
C6	Cement (1 part) + Laterite (3 parts) + Coir (30 wt%)
C7	Cement (1 part) + Laterite (4 parts) + Coir (10 wt%)
C8	Cement (1 part) + Laterite (4 parts) + Coir (20 wt%)
C9	Cement (1 part) + Laterite (4 parts) + Coir (30 wt%)

The composite structures were thus, designed to withstand loads, strong enough to absorb impact without the fibres dissociating from the structure. Both ends of the samples were clipped and pulled apart, while some compressive forces were also applied in bending and compression.

3.4.5 Three-Point Bend Test

This test was used to provide data on the bending modulus of the composite material produced. The ceramic materials formed from the different mortar ratios were each tested, for their strength and bending modulus. The preferred characteristics in the ceramic material are good compressive strength as well as evidence of little to no cracks formed. The ceramic should be hard and durable.

With a span between supports measuring L = 52 mm, equal specimen widths of b = 56 mm and a thickness of d = 28 mm, the equation for calculating the flexural strength of the specimen reduced to $1.77 \times 10^{-3}F$, where F represents the ultimate failure load. The formula for calculating the flexural strength is given by:

$$s = \frac{3FL}{2bd^2} \tag{3.3}$$

where b is the width, d is the thickness of the sample, L is the distance between the two supports.

The formula for calculating the flexural modulus is given by:

$$f = \frac{mL^3}{4bd^3} \tag{3.4}$$

Where L is the span between supports, b is the width, and d is the thickness of the sample. The equation for calculating the. Flexural modulus of the specimen is also reduced to $0.02856M$, where M represents the slope of the initial straight-line portion of the load-deflection curve.

3.4.6 Hardness Test

The samples were tested for hardness using a durometer on the surface of the material. The material should be resistant to corrosion and wear and thus, must be least impacted by the

durometer. The durometer is pressed on different points (Fig. 3.4), at least 5-10 times on the surface of the test samples and the average values were reported.

***Figure 3.4**: The Shore Durometer for Calculating Hardness of the Samples.*

3.4.7 Fracture Test

This test is used to find parameters of the fracture toughness of the composite structure, which is the ability of the material to resist fracture. This test is performed by introducing a flaw at the edge of a sample. Measuring gauges are placed along the crack face, and a load is applied at both ends of the sample, which are clamped, and measurements are read as the crack opens. The fracture toughness of the material is calculated by the formula:

$$K_{1C} = Y\sigma\sqrt{\pi a} \qquad (3.5)$$

Where Y is a geometry parameter, σ is the applied stress (ultimate tensile strength, and a is the crack length. From the values obtained in the fracture tests, the maximum load at fracture can be determined. Calculation of the geometric parameter Y is given by the formula;

$$Y = \frac{a}{w} = 3\frac{(\frac{a}{w})^{\frac{1}{2}}}{2(1+2\frac{a}{w})(1-\frac{a}{w})^{\frac{3}{2}}} \times [1.99 - \left(\frac{a}{w}\right)\left(1 - \frac{a}{w}\right)\left(2.15 - 3.93\frac{a}{w} + 2.7\frac{a^2}{w^2}\right)] \qquad (3.6)$$

Where a is the notch length, and w is the width of the specimen [24].

3.4.8 Compressive Test

The compressive test is performed to obtain values for the compressive strength of the composite material. This test would provide estimates of the force the stove would be able to withstand in compression. The compressive strength is determined by the formula:

$$\sigma_b = \frac{F}{A} \tag{3.6}$$

where F is the maximum load applied before failure and A is the area of the specimen under compression.

3.4.9 Water Absorption

The sample is then tested for its ability to either absorb water. Samples of the composites with different compositions of coconut fibres were then immersed in water for twenty-four hours. The samples were then weighed. The percentage of water absorption was then calculated from the formula:

$$W = \frac{M_2 - M_1}{M_1} \times 100\% \tag{3.7}$$

where W is the water absorption percentage and M_1 and M_2 are the masses of the sample before soaking and after soaking respectively [25].

3.4.10 Bulk Density

The bulk density of the material is also determined using the formula for density:

$$\rho = \frac{m}{V} \tag{3.8}$$

Where $\rho, m\ and\ V$ represent values of density, mass, and volume of the sample and hence, the composite material. This test is carried out on samples of different mortar mix ratios and respective different percentage compositions of coir fibers.

3.4.11 Thermal Conductivity

This test would be necessary to discover the thermal conductivity of the samples and their respective rates of heat loss. The thermal conductivity, k, of the material was calculated after a series of tests and investigations. The formula for calculating thermal conductivity is given as:

$$k = q\frac{L}{A\Delta T} \tag{3.9}$$

where A is the cross-sectional area of the sample, q is the heat rate of flow, L is the thickness of specimen, T is the temperature (in Kelvin).

The thermal conductivity of the composite is determined using the guarded hot plate technique; a mechanism through which conductivity of a material is obtained by placing a solid material between two plates [22]. One plate is heated, and the other is cooled or heated to a lesser extent. The temperature of the plates is monitored and recorded using a Vernier LabQuest 2 (Model LQ2-LE, Vernier Software & Technology, Oregon, United States). Temperatures are monitored until the two plates have a constant temperature. The thickness of the specimen, rate of heat transfer, area of the specimen and peak temperature difference are used as inputs to determine the conductivity of the composite material.

The rate of heat transfer is determined using the formula [22];

$$q = 1000 \times \frac{\Sigma\Delta E}{\Sigma\Delta T} \times \eta, \tag{3.10}$$

Where $\Sigma\Delta E$ is the total power consumption, (kW/h)

$\Sigma\Delta T$ is the duration for temperatures to be constant, (hours)

η is the rated hot plate efficiency given the heating intensity.

3.4.12 Optical Characterization

Images of the microstructure of the different matrix compositions as well as the different percentage compositions of reinforcements were captured for optical characterisation. The images captured can also be used to describe the morphology of the samples, and it also plays indicative roles in determining the mode of failure in samples.

3.5 Fabrication of the Stove

Composites with optimised properties were considered in the fabrication of the stove.

In the process of fabricating the stove, the following steps were implemented in the methodology:

1. **SolidWorks design.**

The finished product is designed using the SolidWorks computer-aided design software. This design is a visual representation of the final product. The model guides the fabrication process and also allows a series of simulation tests to be carried out on the composite material. The design is shown in Figure 3.5.

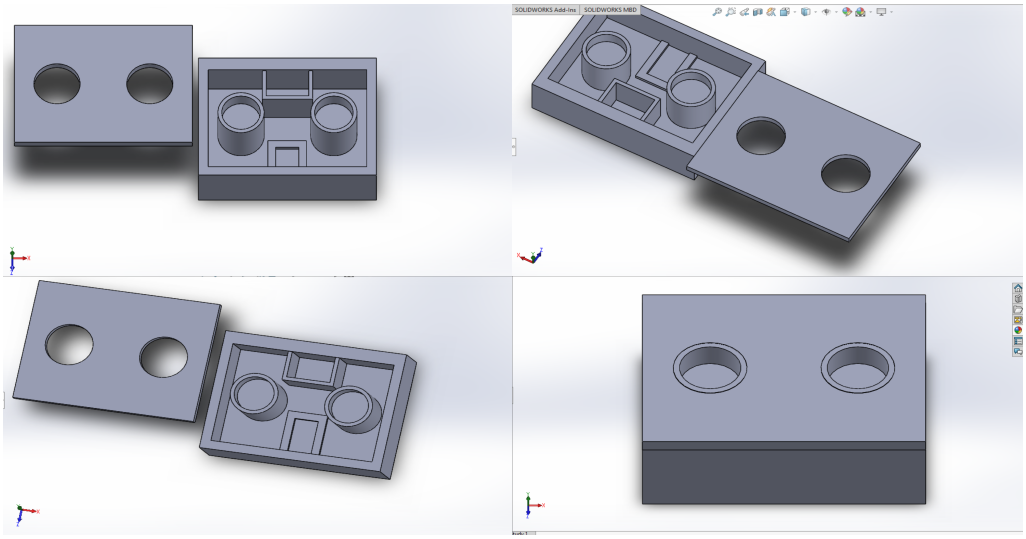

***Figure 3.5**: SolidWorks Module of the Constructed Stove.*

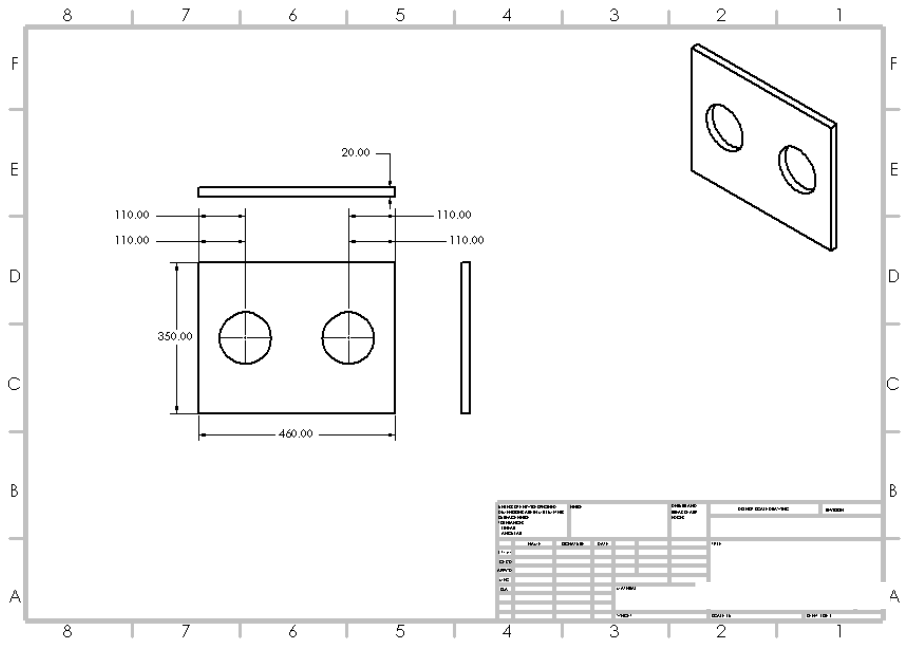

***Figure 3.6**: SolidWorks Sketch of the Stove's Cover.*

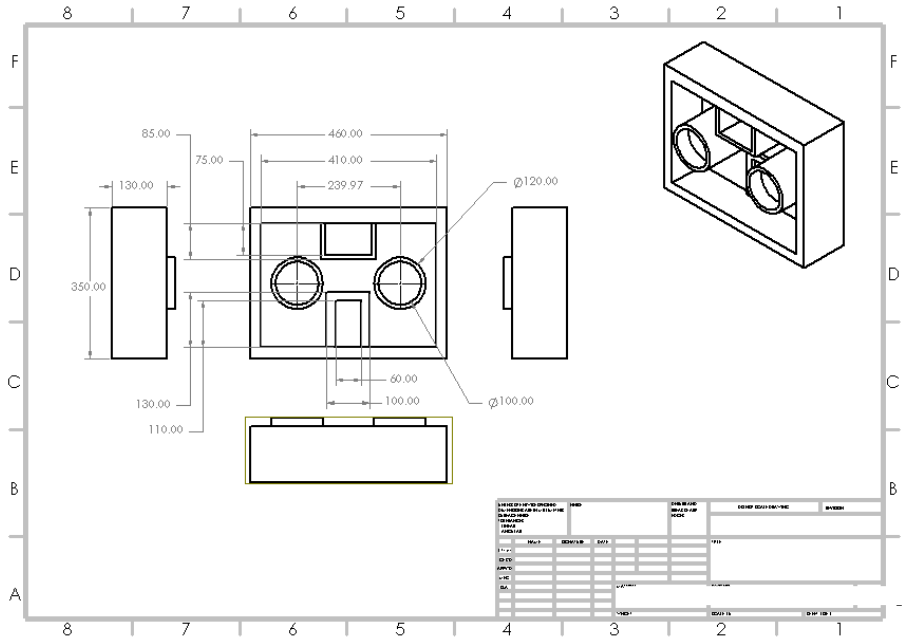

***Figure 7**: SolidWorks Sketch of the Stove's Base*

The SolidWorks model and sketch above in the figure was designed with two components; a base which contains the working elements of the stove and a countertop cover. The stove has a base area of 35cm × 46 cm. The base of the stove was 13 cm high. The stove's cover had the same area as the base and had a height of 2 cm.

2. SolidWorks simulations.

Before the fabrication, a SolidWorks design was completed, while simulations were conducted on the model, to simulate the failure analysis.

The simulation in SolidWorks was carried out using the software's Thermal Study and Load analysis features. The study was conducted to visualise the heating effects of the heating elements on the stove's properties and components. The output of the simulation would show a thermal and structural analysis of the stove when in full operation.

The prototype constructed were then tested with the electrical elements installed. The entire system was simulated for performance. Heating effects of the stove were realised through boiling a volume of water within an estimated time frame. The efficiency of the stove was also calculated as:

$$\eta = \frac{W_{out}}{W_{in}} \times 100,$$

Where W_{out} and W_{in} are the power input into the heating elements and power output measured.

Chapter Four

Results and Discussion

4.1 Tensile Test Results

For the tensile tests, the samples were assigned a nomenclature for easy identification. The fibres were differentiated based on different sample soaking times and different solutions they were soaked in. The table explaining the nomenclature is given below;

***Table 4.1**: Nomenclature of samples for tensile tests*

Fibre	Modification
F1	Soaked in 5% NaOH for 6 hours
F2	Soaked in 5% NaOH for 12 hours
F3	Soaked in 5% NaOH for 18 hours
F4	Soaked in 5% NaOH for 24 hours
F5	Soaked in 6% NaOH for 6 hours
F6	Soaked in 6% NaOH for 12 hours
F7	Soaked in 6% NaOH for 18 hours
F8	Soaked in 6% NaOH for 24 hours
F9	Soaked in 7% NaOH for 6 hours

Fibre	Modification
F10	Soaked in 7% NaOH for 12 hours
F11	Soaked in 7% NaOH for 18 hours
F12	Soaked in 7% NaOH for 24 hours
F13	Soaked in 8% NaOH for 6 hours
F14	Soaked in 8% NaOH for 12 hours
F15	Soaked in 8% NaOH for 18 hours
F16	Soaked in 8% NaOH for 24 hours

The summary of results from the tensile tests is summarised in the table below (Table 4.1).

***Table 4.2**: Results from tensile tests of samples.*

Sample	Average Diameter	Average Strain at Break	Average Peak Load	Average Peak Stress	Average Modulus
F2	1.165	0.2575	0.045	0.06	0.7905
F3	1.315	0.1655	0.044	0.035	1.085
F4	1.55	0.1025	0.023	0.012	0.3505
F6	0.76	0.2655	0.0315	0.045	0.091
F7	0.795	0.2235	0.0389	0.1	1.665
F8	0.915	0.239	0.051	0.1	1.368
F10	1.335	0.1805	0.0355	0.025	0.5715

Sample	Average Diameter	Average Strain at Break	Average Peak Load	Average Peak Stress	Average Modulus
F12	1.62	0.1755	0.0415	0.02	0.409
F14	1.49	0.2585	0.0425	0.025	0.5795
F15	0.74	0.257	0.036	0.1	1.162
F16	1.105	0.175	0.0375	0.065	1.1235

The table above reports averaged values of the diameter, strain at break, peak load, peak stress and modulus. Unfortunately, the results in the table did not show any consistent trend in variations. The absence of a trend can be attributed to various factors including the inconsistency in several strands used during the tests. The extensometer's dimension requirements did not allow for single strands to be tested, and hence multiple strands had to be used. This introduced anomalies in graphs and properties of the tensile tests.

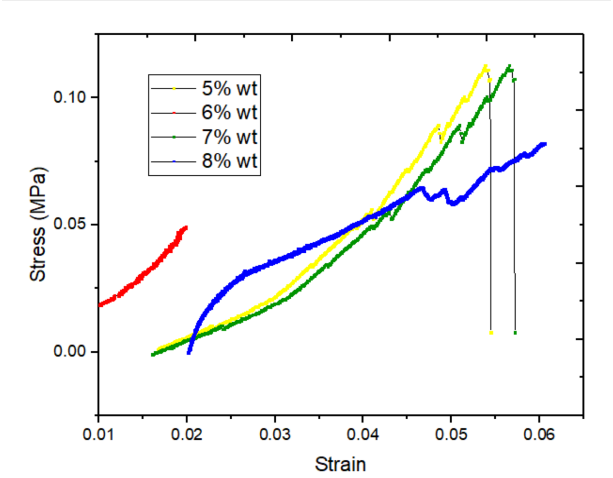

***Figure 4.1**: Plots of Tensile Modulus of Fibers Soaked in Different Concentrations of NaOH.*

Fibre Young's modulus is graphically presented (Fig. 4.3). The best result for Young's modulus was obtained with 6 wt% for 18 h treatment. There was also a second-best result obtained at 8 wt% NaOH. Among all, 7 wt% of NaOH in solution recorded the least value of Young's modulus.

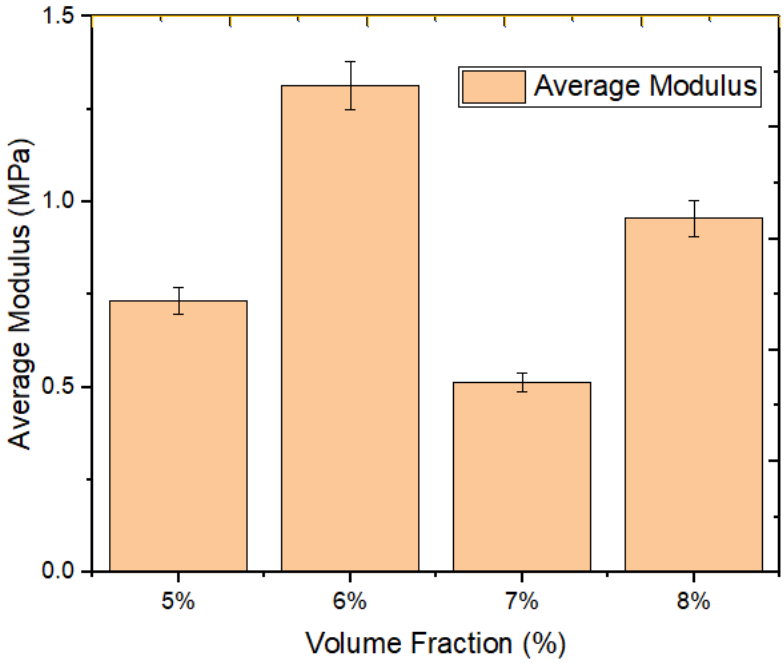

***Figure 4.2**: Average Elastic Modulus of Fibers with Different Concentrations of NaOH*

Figure 4.3 showed the results of the stress-strain curves for treated fibres after being soaked in the different NaOH concentrations. On the other hand, Figure 5.4 shows the stress-strain curves for treated fibres at different durations when incubated in 6 wt% solutions. The duration spent in the solution were compared with each other to determine the optimum amount of time the fibres should be soaked in the solution.

The results show that the fibres soaked in 6 wt% NaOH solution for 18 h had the highest strength of about 0.15 MPa, followed by 24 h with a strength of 0.063 MPa.

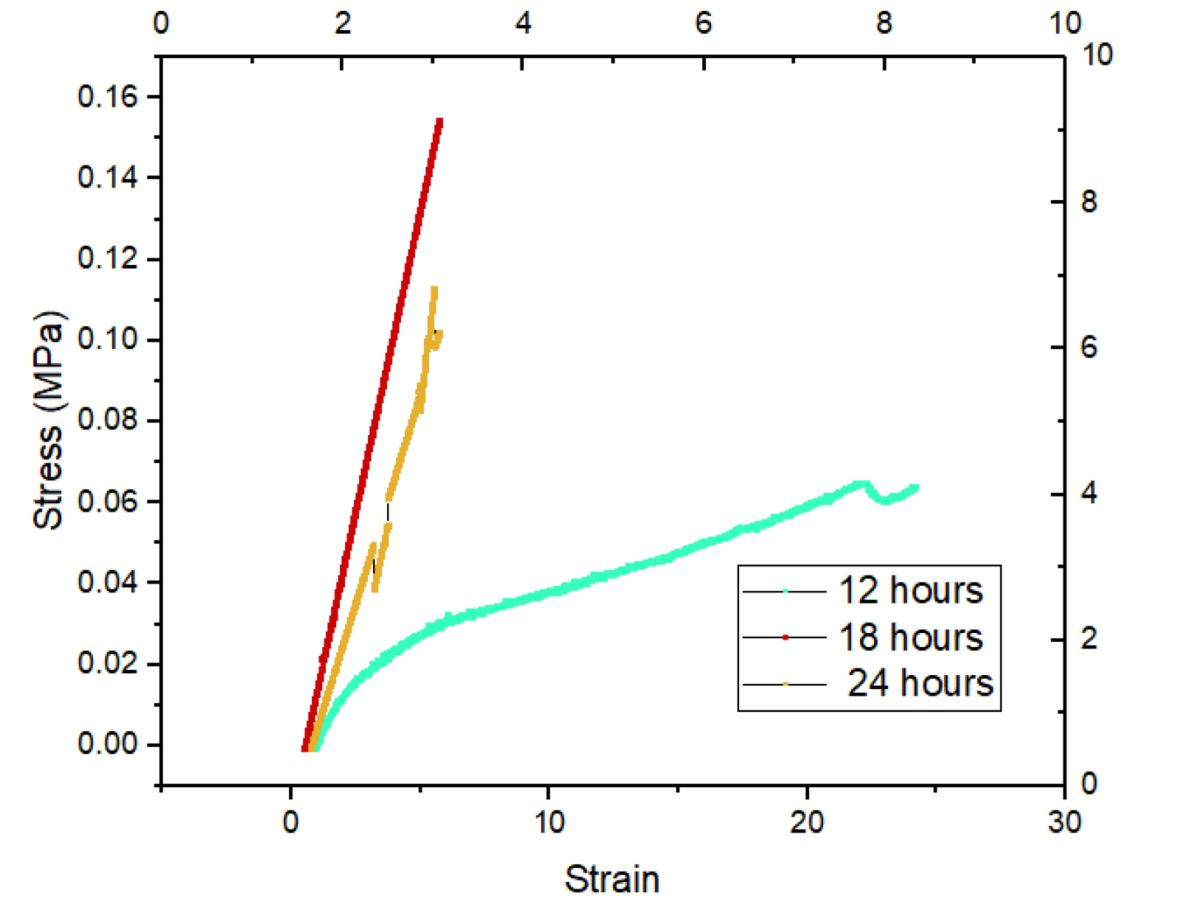

***Figure 4.3**: Comparison of 6 wt% fibres by duration.*

Fibres from the 6 wt% at 18 h were then used to create Earth-based composite as shown (Fig. 4.4). The cement-laterite ratio at 1:2, 1:3 and 1:4 were then used to build the composites.

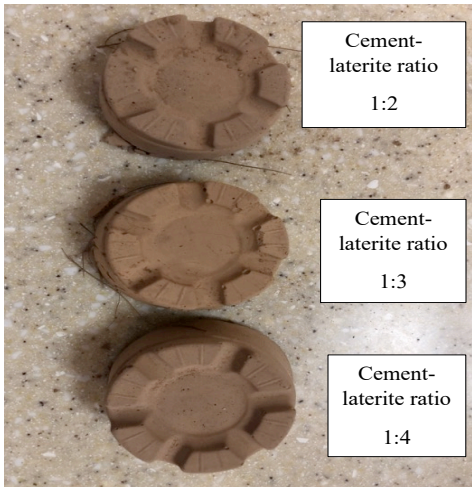

***Figure 4.4**: Ceramic Samples Made in Matrix Ratios 1:2, 1:3 and 1:4.*

Fibre Pullout

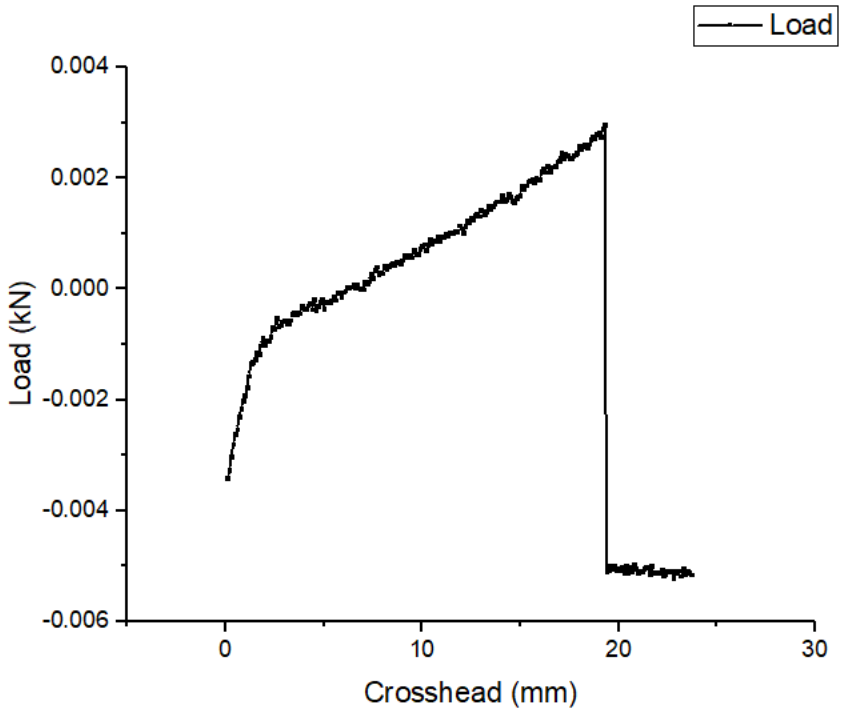

***Figure 4.5**: Load-displacement graph after fibre pullout test.*

Figure 4.5 showed the load-displacement graph obtained from the fibre pullout test. The graph shows the two distinct phases of the entire process; the debonding process and the fibre pullout process. From the graph, the debonding shear strength was determined. The peak load was recorded at 0.0031 kN. From Equation 3.1,

$\tau_d = \frac{F_d}{2\pi r l_e}$.

With an embedded length of 19 mm and a fibre radius of 0.15mm, the debonding shear stress becomes $\tau_d = \frac{0.0031}{2\pi \times 0.15 \times 19} = 1.731 \times 10^{-4}\ MPa$.

The result is used to calculate the critical fibre length using Equation 3.2;

$l_c = \frac{\sigma d}{2\tau}$.

With an ultimate tensile strength of 0.042, critical length becomes

$l_c = \frac{0.042 \times 0.3}{2(1.731 \times 10^{-4})} = 36.39\ mm$.

4.2 Hardness

The hardness test carried out on nine different sample specimens is presented (Table 4.2). For three different mix ratios and three different fibre compositions within each of the three mix ratios. The hardness values were derived from reading the scope of the durometer used. The averaged values of the test recorded (in HD)

For a composite made with ten wt% fibre, the hardness decreases with increase in fibre composition. A lower composition of fibre corresponds to a higher composition of the matrix. This low fibre composition would account for a higher hardness value. However, the highest hardness value obtained was 62 HD, observed in the 1:2 matrix mix with 10% fibre reinforcement. For the case of 20 wt%, the HD increased from 50 (at 1:2) to 60 at (1:3). The trend shows an increase in the hardness with an increase in fibre volume which caused a reduction in HD from 50-60 HD. However, this result deviated from 10 wt%. The process of

curing the sample beyond five days would possibly increase HD beyond the current data, which were obtained after five days of moulding. This is subject to future investigation.

Table 4.3: Hardness values (HD) of samples.

Mortar Ratio/%age composition	10%	20%	30%
1:2	62	50	49
1:3	59	51	42
1:4	46	60	59

4.3 Three-Point Bend Test

Force-displacement graphs of the tested samples are shown below in Figure 4.6. The three-point bend tests yielded results for analysis on both the flexural strength and the flexural modulus of the samples created.

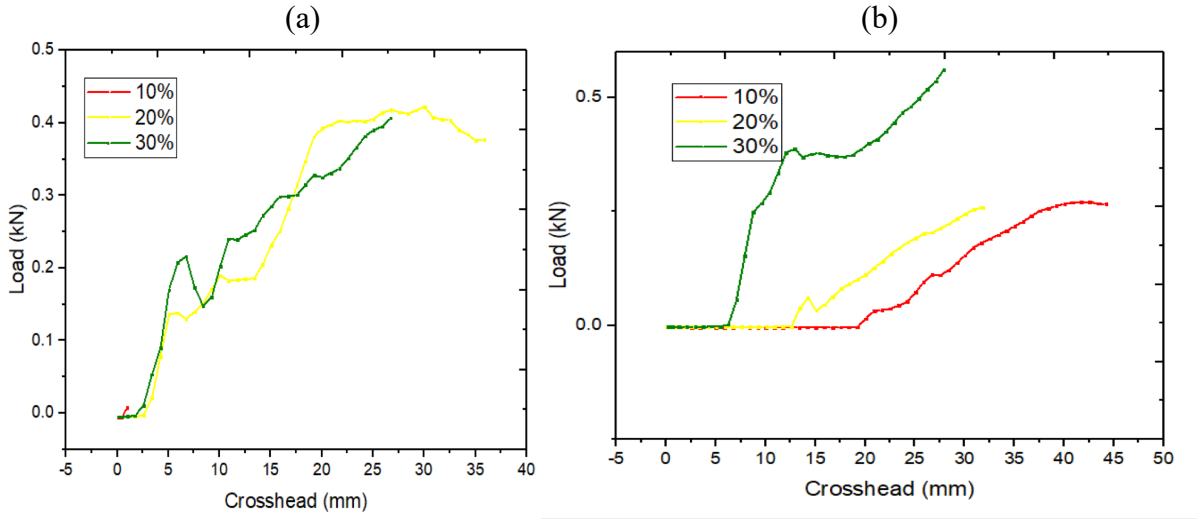

(c)

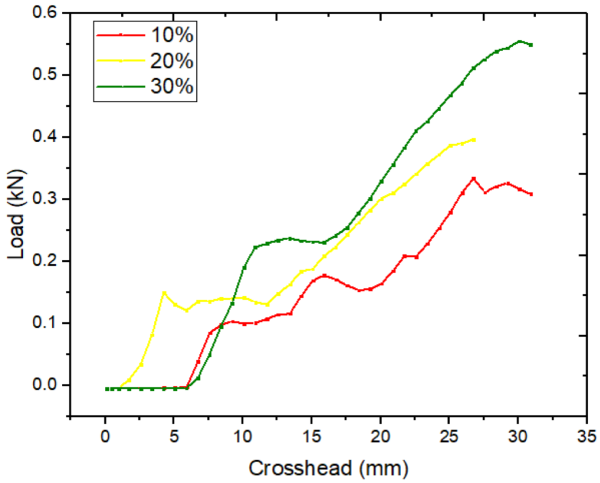

***Figure 4.6**: Force-Displacement Graphs of Samples after Three-Point Bend Tests: (a) cement to laterite ratio 1:2, (b) cement to laterite ratio 1:3, and (c) cement to laterite ratio 1:4.*

***Table 4.4**: Flexural strength of samples (MPa)*

	10%	20%	30%
1:2	-	0.6992	0.7081
1:3	0.5558	0.6761	0.9717
1:4	0.4071	0.4354	1.0159

The flexural moduli for the samples were plotted in groups against each other (Fig. 4.6). In one group, samples with the mortar ratio 1:2 were compared. In the second group, samples with mortar ratio 1:3 were compared and likewise, in the third group, samples with the mortar ratio of 1:4 were compared.

***Table 4.5**: Flexural modulus of samples (GPa)*

	10%	20%	30%
1:2	-	0.00036557	0.00042871
1:3	0.00033562	0.00040958	0.00058541
1:4	0.00030633	0.00026475	0.0006179

The flexural modulus of the samples was obtained from the graphs presented in Figure 4.6. The slopes of the curves were recorded by the MTS software and collated into Formula 3.4. The calculated moduli have been recorded in Table 4.4 and plotted in bar charts in Figure 4.7. The trend of flexural moduli increases with an increasing amount of laterite in the composite material. It can also be observed that the flexural modulus increases with the increasing volume fraction of fibre reinforcements.

This trend could be explained because a higher percentage of cement in the composite structure would harden the sample and reduce its flexural ability. In addition to this, higher fibre content would increase the flexural properties of the sample.

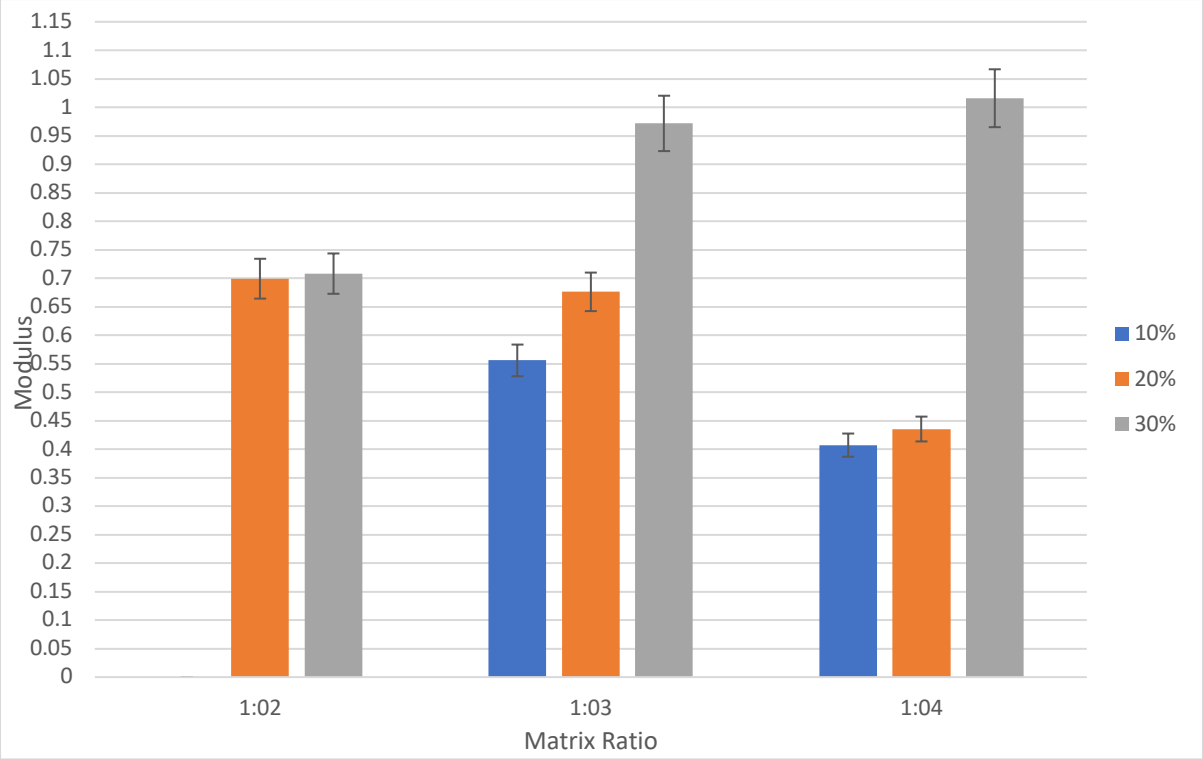

Figure 4.7: *Comparison of Flexural Moduli by Volume Fraction.*

It was observed that in all three sample groups, the samples reinforced with a 30 wt% fibre ratio had the highest flexural modulus as shown in Figure 4.5.

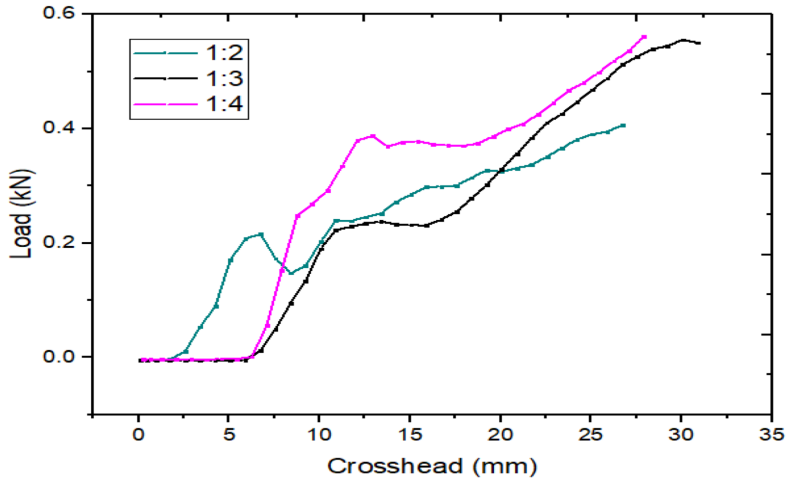

Comparison of different mortar ratios with 30% fiber reinforcement

Figure 4.8*: Comparison of mix ratios of 30% fibre reinforcement.*

Table 4.4 shows that mortar ratio 1:4 produces the highest flexural strength and modulus. The flexural strength is weakest at a mortar ratio of 1:2. These statistics can be inferred from — the plot in Figure 4.6.

4.4 Optical Characterization

The microscopic images of the samples were captured using the digital microscope U 800X camera. Images were also captured of the sample with reinforcements which had failed during a three-point bend test.

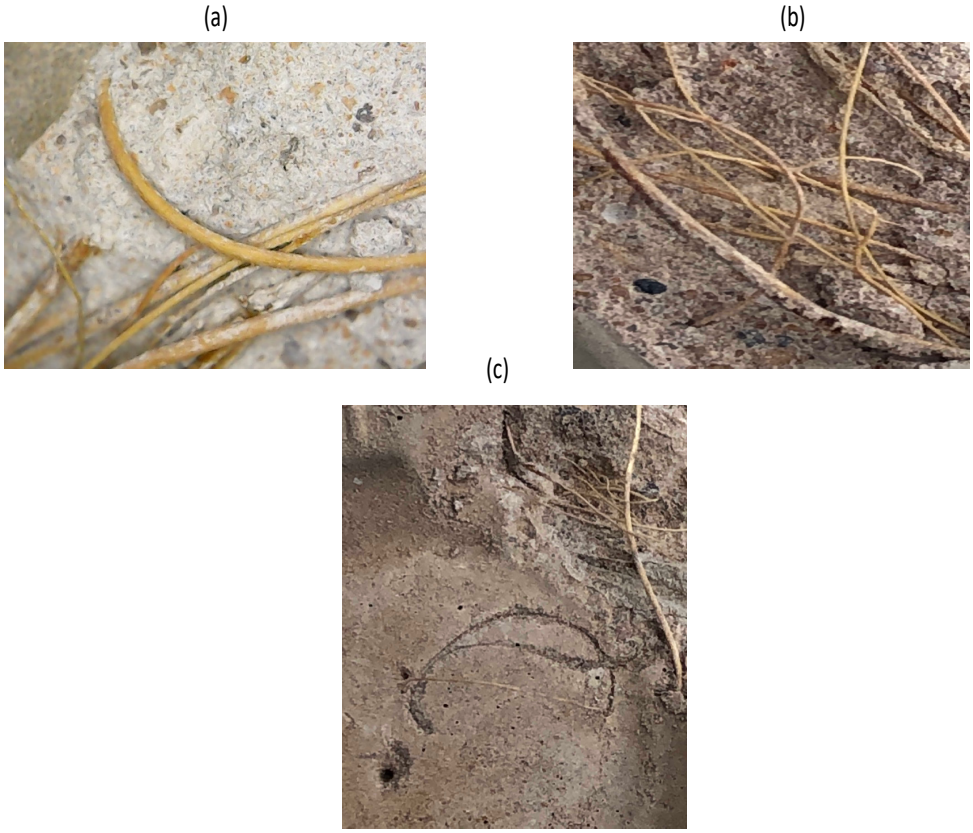

***Figure 4.9**: Internal view of composite sample with matrix ratio (a) 1:2 (b) 1:3 (c) 1:4*

Images recorded with the microscopic camera also revealed the growth of pores and cracks within the samples which were dried without curing. These samples are shown in Figure 4.10.

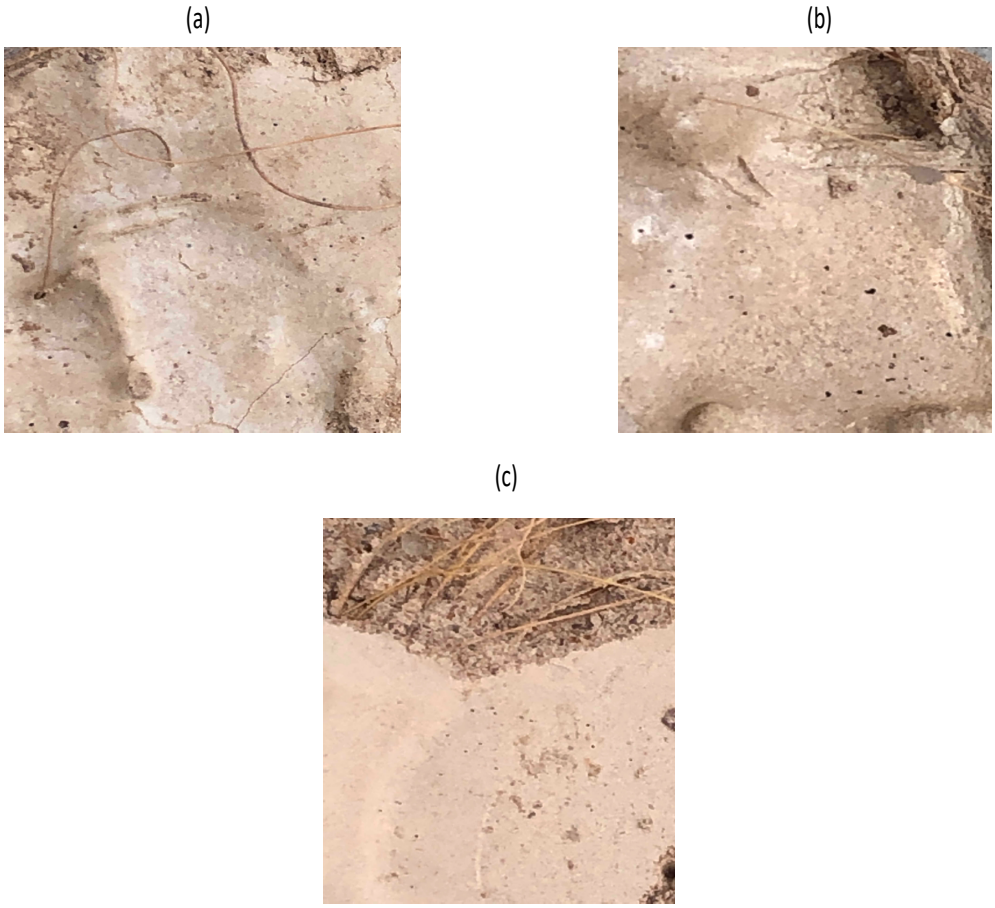

***Figure 4.10**: Images showing the development of pores and cracks in samples with matrix ratio (a) 1:2, (b) 1:3 and (c) 1:4*

Images were also captured of samples which were cured for four days. The images are presented in Figure 4.11.

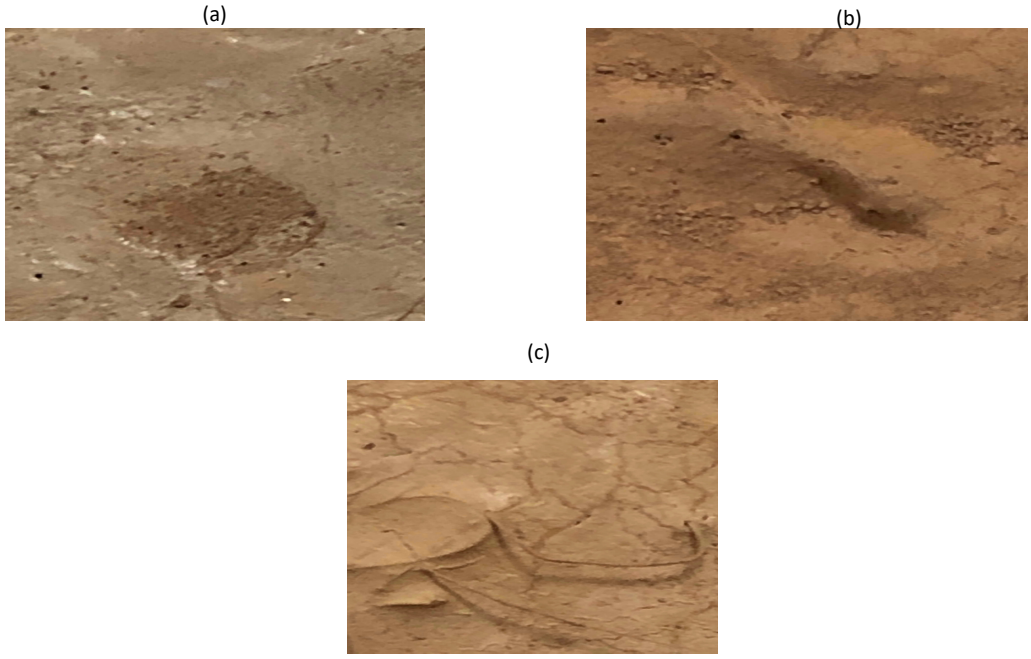

***Figure 4.11**: Images of (a)1:2, (b) 1:3 and (c) 1:4 samples which were cured for four days.*

The cured samples developed thin film-like surfaces due to the presence of moisture on the surface during the process of drying. These surfaces fill the pores created by shrinking during the hardening process.

4.5 Water Absorption

The samples used in the hardness test were soaked in clean water for twenty-four hours. Each sample was weighed, and the percentage of water absorption was recorded. The table below shows (Table 4.6) the recorded results of the water absorption test. It was observed that water absorption increased with fibre ratio. Thus, the percentage of swelling increased from 10-30%. On the other hand, the cement to laterite ratio also caused a degree in water absorption with an increase in laterite ratio.

Table 4.6: Water absorption of samples.

Mortar Ratio/ %age Composition	10%	20%	30%
1:2	9.2%	11.1%	11.6%
1:3	9.1%	10.3%	10.7%
1:4	7.7%	8.4%	9%

4.6 Fracture Toughness

The fracture toughness of one sample was determined from Equation 3.5. From the formula, the parameter Y is calculated as a geometric parameter and a function of the dimensions of the specimen under testing. With a specimen width of 54 mm and a notch length of 5 mm, Y was found to be;

$$Y = \frac{a}{w} = 3\frac{(\frac{a}{w})^{\frac{1}{2}}}{2(1+2\frac{a}{w})(1-\frac{a}{w})^{\frac{3}{2}}} \times [1.99 - \left(\frac{a}{w}\right)\left(1-\frac{a}{w}\right)\left(2.15 - 3.93\frac{a}{w} + 2.7\frac{a^2}{w^2}\right)]$$

$$= 3(0.1485) \times [1.99 - 0.084(2.15 - 3.93(0.0926) + 0.0231)]$$

$$= 0.4455 \times [1.99 - 0.084(1.809)]$$

$$= 0.8188$$

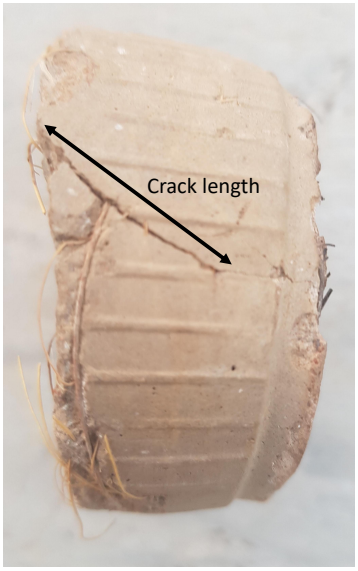

***Figure 4.12**: An image of the specimen after fracture testing.*

Figure 4.8 shows the crack developed after stress was applied to a notch created on the specimen. A stress of 5MPa was applied to the specimen, which yielded an increase in the notch length by 27 mm.

Fracture toughness is therefore calculated using Equation 3.5.

$$K_{1C} = (0.8188)(5)\sqrt{\pi(0.027)} = 1.19MPa\sqrt{m}.$$

4.7 Thermal Conductivity

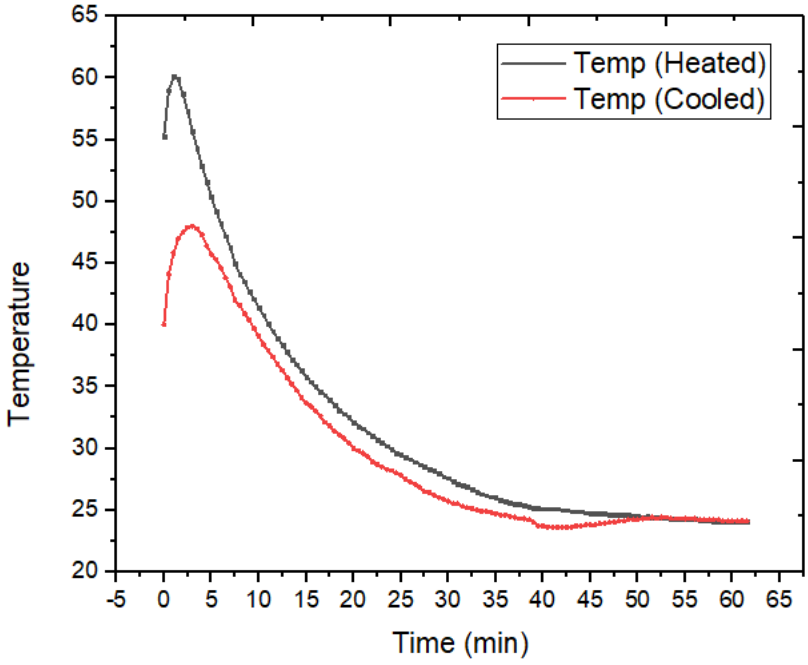

***Figure 4.13**: Plot showing temperatures of both plates against the time taken to reach constant temperature.*

The thermal conductivity was found using the guarded hot plate method. One surface of the sample was heated while the other surface was in contact with the cooler plate. The hotter plate was heated using an AKO Elektrogerate KP515 electric hotplate. The temperatures were observed to be constant after 61.5 minutes. With a rated efficiency of $17{,}726 \times 10^{-3}$ moreover, the power consumption of 0.12 kW/h, q is calculated from Equation 3.10 to be

$$q = 1000 \times \frac{0.12}{1.025} \times 17{,}726 \times 10^{-3} = 2.075\ kW\ .$$

The cross-sectional area of the specimen was $2.123 \times 10^{-3}\ m^2$ and had a thickness of 34 millimeters. The temperature of the heated plate and cooled plate at the beginning of the experiment were measured at 55.3℃ and 40.0℃ respectively ($\sim 328.3K\ and\ 313K$). The temperature difference is hence recorded as $328.3 - 313 = 15.3K$.

From Equation 3.9,

$$k = 2.075 \times \frac{0.034}{(2.123 \times 10^{-3}) \times (15.3)} = 2.171 \frac{W}{mK}.$$

4.8 SolidWorks Design and Simulation

The prototype model was first developed for testing and simulations. The prototype was designed in a SolidWorks assembly. Static loads and thermal loads were applied to the model to simulate its performance under the normal boundary conditions which are defined by mean environmental conditions during operation.

Under static loading, the model was subjected to a force of 1000N and simulation on displacement, impact strain and impact stress were conducted — the SolidWorks. The simulation yielded the following results displayed in Figure. 4.14.

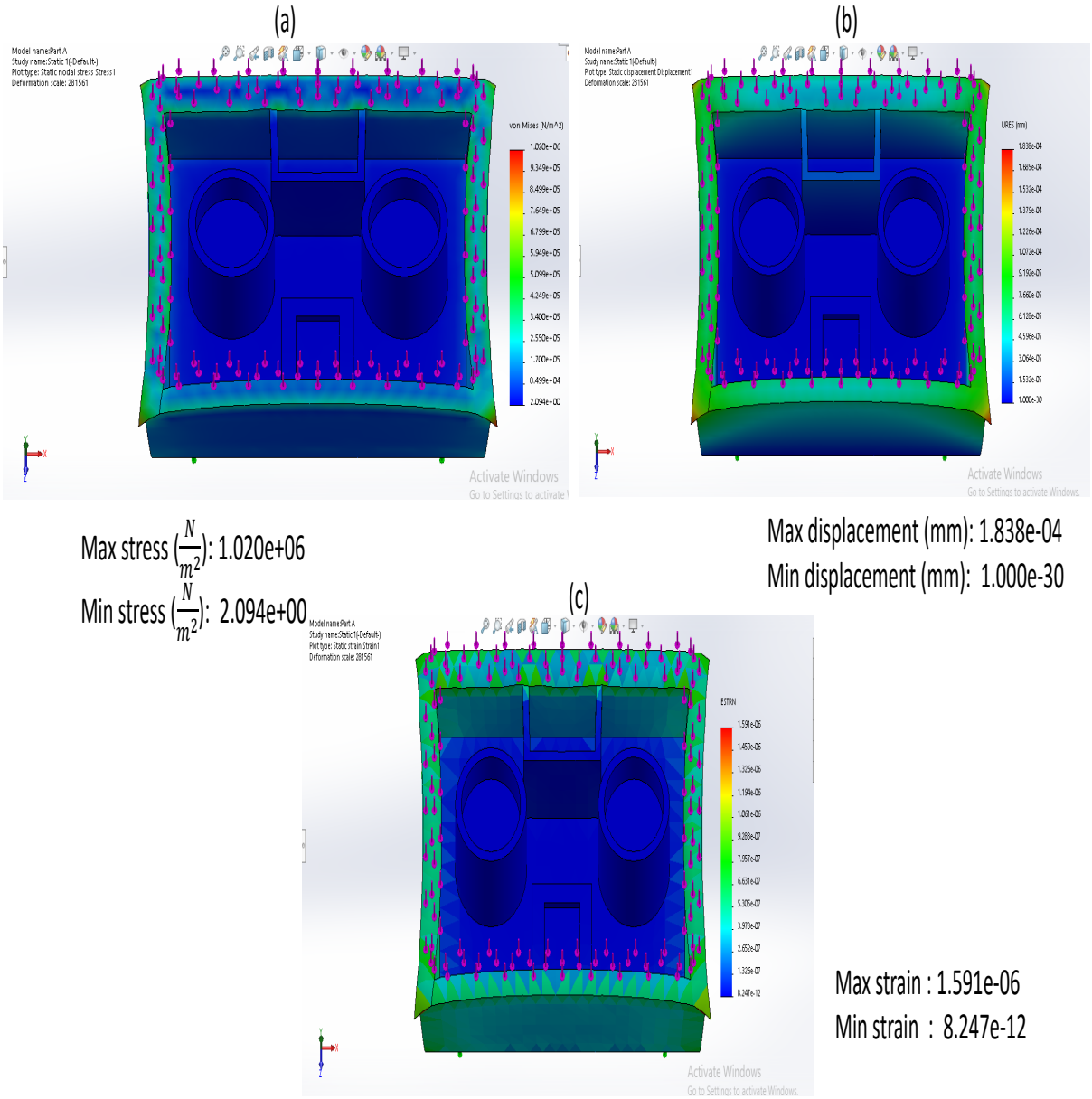

***Figure 4.14**: Simulation results of the SolidWorks model under (a) stress analysis, (b) displacement and (c) strain analysis.*

The thermal performance of the stove was also simulated in SolidWorks. A heat energy output of 1000W was defined as the boundary condition for the heat energy transmitted by the heating elements of the stove. The temperature being emitted from the heating elements was

approximated at 700K (426.85℃). The thermal study simulation yielded the following result presented in Figure 4.10.

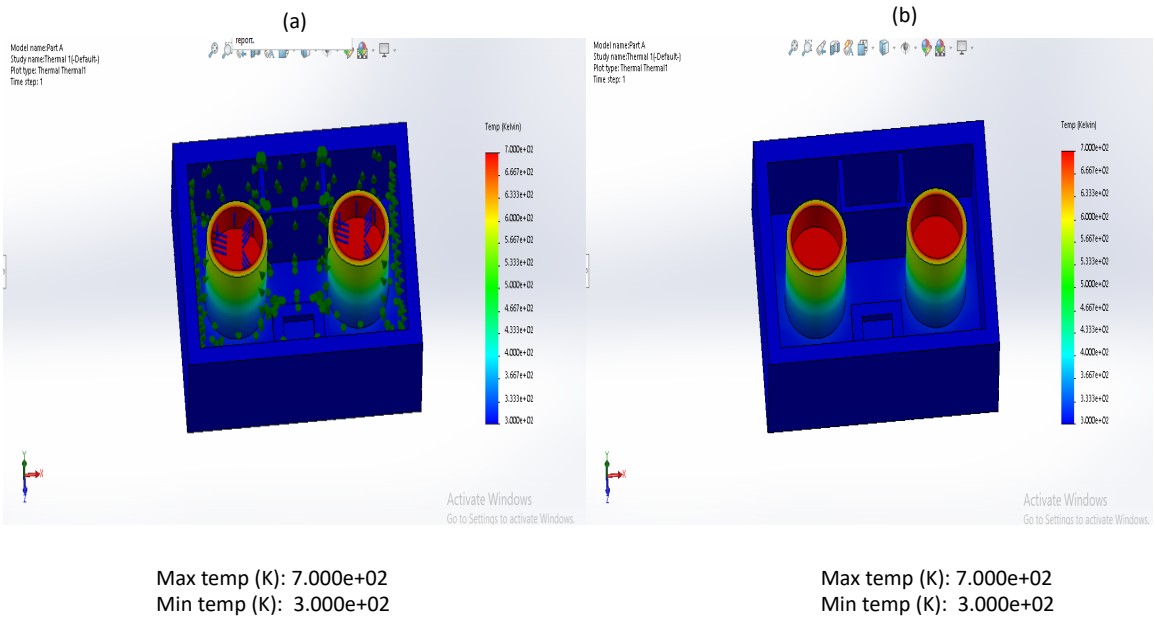

***Figure 4:15**: (a) The results of the thermal study showing thermal loads on the model. (b) the thermal study with loads hidden, indicating temperatures at different regions of the model.*

The results from the static loading indicate that a force of 1000N is enough to slightly alter the shape of the stove's base near the cover, but not enough to fail the material. Under thermal studies, the temperature within the hotplates was defined at 700K to simulate the temperature produced by the heating elements during cooking. The thermal studies revealed the behaviour of heat transfer within the stove, spreading from the area of heat generation within the hotplates outward within the stove. The temperatures can be read from Figure 4.15. The higher temperatures can be read to be contained within the heated area. The walls of the stove, as well as most of the internal components, can be seen to be relatively unaffected by

the heat generated by the hotplates. Temperatures at the walls of the stove can be read to be about 300K, which is about standard room temperature.

With the ability to withstand an impact force of 1000 N without failing and a surface temperature of 300K (26.85℃), the stove is fit to pass thermal and static loading tests. The stove can, therefore, be concluded to be safe for use and operation.

Chapter Five

Conclusions Remarks, Limitations and Recommendations

5.1 Conclusions

The tensile tests performed on the fibres were carried out with MTS Tensile machine. In total, sixteen different samples were tested for their Young's Modulus and their tensile strength. The results showed that the fibres soaked in 6 wt% sodium hydroxide recorded higher values for their elastic modulus. Following the results, the different durations the fibres incubated in the NaOH solutions were also compared. After comparison, it was observed that the fibres soaked for 18 h had higher values of elastic modulus, ranging from 1.058 to 1.665 MPa. For the above reasons, the reinforcement selected for the project was coir fibres soaked in 6 wt% sodium hydroxide solution for 18 h.

The fibre pull-out test was necessary for determining the debonding shear stress of $1.731 \times 10^{-4}\ MPa$ when coir fiber is used in a laterite-cement mix. The critical length determined from the fiber pullout test was a fiber length of 36.39mm.

The hardness tests were performed on nine samples which differ in volume fraction in terms of fibre and matrix mix ratios. The hardness test performed yielded results that demonstrated that the hardest material was a mix ratio of 1:2 (one-part cement, two-parts laterite), which included ten wt% volume fractions of the selected fibres. Trends observed they showed that hardness decreased with the increasing volume fraction of fibres. The hardness decreases because the harder matrix in the composite is replaced by more of the fibre is used. Hardness, however, was not used as a determining factor for the best composite sample due to how closely values compared to each other.

The three-point bend tests provided data for calculating the flexural strength and flexural modulus of the samples. Results from the tests showed that the average values for the flexural strength and flexural modulus were highest in the mix ratio of 1:3. Flexural strength, as well as flexural modulus, was observed to increase with an increase in the volume fraction of fibre reinforcements.

Optical characterisation revealed that there were a few, negligible differences between the different samples. The images, however, showed the advantage of curing. Curing appears to increase the strength of the samples and reduce the number of pores and cracks generated during the hardening process.

The water absorption test also revealed an increase in absorption with a corresponding increase in fibre ratio. Higher laterite to cement ratio also improved water absorption abilities of samples.

The samples responded with better mechanical properties when a volume fraction of 30% fibre reinforcement was used. These samples were therefore used for fracture toughness and thermal conductivity tests. Due to a higher averaged value of flexural strength and flexural modulus in the samples made with a mix ratio of 1:3, the samples selected for fabrication were made of a composition of one (1) part cement and three (3) parts of anthill sand.

The thermal conductivity test was performed on the selected composite using a guarded hot plate technique. The conductivity test showed that the ceramic composite sample had a conductivity coefficient of $2.171\frac{W}{mK}$, a value that is comparably desirable in the case of other materials used to construct the bodies of stoves.

The fracture toughness of the sample was calculated to be 1.19 $MPa\sqrt{m}$, which indicates a higher fracture toughness value than conventional ceramics. The prototype model was simulated in SolidWorks for failure analysis and thermal studies, instead of applying forces

to the actual prototype. The simulations saved time and allowed for various results given different boundary conditions. After analysis in SolidWorks, the stove was shown to possess high strength and a high resistance to heat transfer within the stove, withstanding a force of 1000N. without fail and maintaining room temperature along its walls and surface while 1000W of electrical power heated up hotplates to a temperature of 700K.

5.2 Limitations

The project has faced a variety of limitations. A significant number of the limitations faced were linked to the availability of facilities and apparatus for the project.

In addition to this, the machine for carrying out tensile tests carries specifications which do not allow for calculations on diameters lesser than 0.58 mm. One strand of coir fibre was lesser than the given diameter. For the tests to be performed, strands had to be braided with each other which distorted values during the tensile tests, since different strands failed at different strengths.

Additionally, the absence of apparatus made it unable to conduct compressive tests.

Fabrication of the stove proved difficult, as the mechanical workshop in Ashesi University has not yet been equipped with structures to aid in fabrication and moulding of ceramic units. The first product was not designed accurately by the SolidWorks model. This occurred because the inner components of the stove could not be moulded accurately, given the unavailability of cylindrical moulds in the workshop.

5.3 Recommendations for Future Work

For future works, I would recommend a broader investigation of fibres which may not be readily available in Africa but having similar or better qualities compared to coir fibre. Possibly, different solutions could be used for the fibre treatment process to investigate the effects of chemical compositions on the properties of fibres.

It should also be recommended that apparatus with flexible dimension restraints should be used. The constraints placed on test samples due to machine requirements can introduce inconsistencies in data and reduce the genuine nature of experiment data.

Future works should also incorporate the investigation of different arrangement and orientation of fibres in the matrix.

The prototype of the fabricated stove should also be modified in its aesthetic appeal. Professional ceramic moulding would be preferred if possible, for a clear structure.

Future works could also investigate the maximum allowed volume fraction of fibres used for reinforcements.

Compressive tests should be carried out as well on samples to evaluate the compressive strength of the material.

References

[1] M. Szukzewski, "Field Tests of the Hotpot, A New Solar Cooker in West Africa," *Solar Household Energy,* p. 1, 20 October 2006.

[2] M. Amoah, O. Marfo and M. Ohene, "Firewood consumption pattern, availability and coping strategies adopted to mitigate firewood scarcity: a case of rural households in Ghana," *Forests, Trees and Livelihoods,* vol. 24:3, no. DOI: 10.1080/14728028.2015.1052854, pp. 202-218, 2015.

[3] M. Balat, "Solar Technological Progress and Use of Solar Energy in the World," *Energy Sources, Part A: Recovery, Utilization, and Environmental Effects,* vol. 28:10, no. DOI: 10.1080/009083190953409, pp. 979-994, 2006.

[4] F. K. Forson, F. O. Akuffo and N. M. A. A., "Natural convection solar crop-dryers of commercial scale in Ghana: design, construction and performance," *International Journal of Ambient Energy,* vol. 17:3, no. DOI: 10.1080/01430750.1996.9675231, pp. 123-130, 1996.

[5] H. Aigbe and S. Oluku, "Depleting Forest Resources of Nigeria and Its Impact on Climate," *Journal of Agriculture and Social Research,* vol. 12, 2012.

[6] Ghana Statistical Service, "Ghana Living Standards Survey 5," 2008.

[7] Ghana Statistical Service, "Ghana Living Standards Survey 6," 2014.

[8] J. Bonan, S. Pareglio and M. Tavoni, "Access to Modern Energy: a Review of Impact Evaluations," *Fondazione Eni Enrico Mattei,* pp. 5-8, 2014.

[9] IEA, "World Energy Outlook 2013," International Energy Agency, Paris, 2013.

[10] A. Niyibizi, SWOT Analysis for Renewable Energy in Africa Challenges and Prospects, Claeys & Casteels Law Publishing.

[11] A. Zahedi, "How Expensive is Grid-Connected Solar Photovoltaic in Marrakesh?; An Economic Analysis," *Crown,* pp. 2-5, 2015.

[12] H. D.Dande and S. D. Markande, "Solar Based Induction Heating System," *IEEE,* pp. 2-3, 2014.

[13] Global Alliance for Clean Cookstoves, "Handbook for Biomass Cookstove Research, Design and Development; A Practical Guide To Implementing Recent Advances," *MIT D-Lab,* pp. 36-43.

[14] T. Chineke, O. Nwofor and O. U.K., "Optimal benefits of utilizing renewable energy technologies in Nigeria and the CIBS quadrangle: a review," *Bayero Journal of Pure and Applied Sciences,* pp. 2-3, 2010.

[15] Berteaud, A. and Badot, J. (1976). High-Temperature Microwave Heating in Refractory Materials. *Journal of Microwave Power*, 11(4), pp.315-2320.

[16] Kuntz, J., Zhan, G. and Mukherjee, A. (2004). Nanocrystalline-Matrix Ceramic Composites for Improved Fracture Toughness. *MRS Bulletin*, 29(01), pp.22-27.

[17] Kuntz, J., Zhan, G. and Mukherjee, A. (2004). Nanocrystalline-Matrix Ceramic Composites for Improved Fracture Toughness. *MRS Bulletin*, 29(01), pp.22-27.

[18] Homeny, J. and Vaughn, W. (1987). Whisker-Reinforced Ceramic Matrix Composites. *MRS Bulletin*, 12(07), pp.66-72.

[19] Ali, M. Claisse.info. (2019). [online] Available at: http://www.claisse.info/2010%20papers/k13.pdf [Accessed 1 Apr. 2019].

[20] Thomas, G. (2019). *International Year of Natural Fibres 2009*. [online] Naturalfibres2009.org. Available at: http://naturalfibres2009.org/en/index.html [Accessed 1 Apr. 2019].

[21] Baruah, P., and Talukdar, S. (2007). "A comparative study of compressive, flexural, tensile and shear strength of concrete with fibres of different origins." Indian Concrete Journal, 81(7), 17-24.

[22] Tpm.fsv.cvut.cz. (2019). [online] Available at: http://tpm.fsv.cvut.cz/student/documents/files/BUM1/Chapter16.pdf [Accessed 21 Apr. 2019].

[23] Callister, W. (2019). *Materials Science and Engineering*. New York: Wiley.

[24] Kolawole, F., Olugbemi, O., Kolawole, S., Owa, A. and Ajayi, E. (2017). Fracture Toughness and Strength of Bamboo-Fiber Reinforced Laterite as Building Block Material. *Universal Journal of Materials Science*, 5(3), pp.64-72.

[25] B. Das, *Soil mechanics*, 7th ed. New York: Oxford University Press, 2016, p. 7.

[26] K. Olusola, E. Olanipekun, O. Ata and O. Olateju, "Studies on termite hill and lime as a partial replacement for cement in plastering", *Building and Environment*, vol. 41, no. 3, pp. 302-306, 2006. Available: 10.1016/j.buildenv.2005.01.034.

Appendix

Appendix A

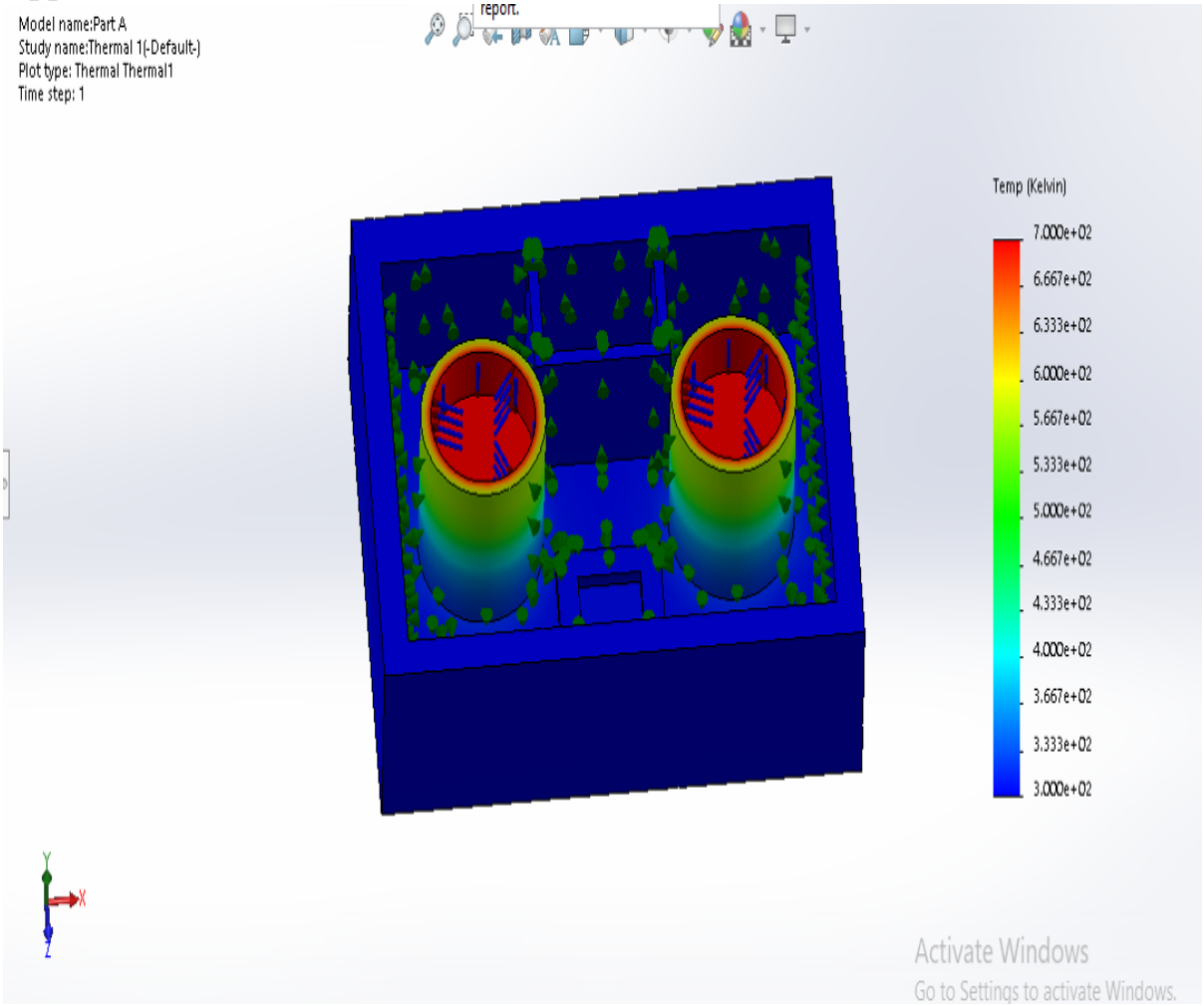

Thermal Simulation showing thermal loads on the stove.

Appendix B

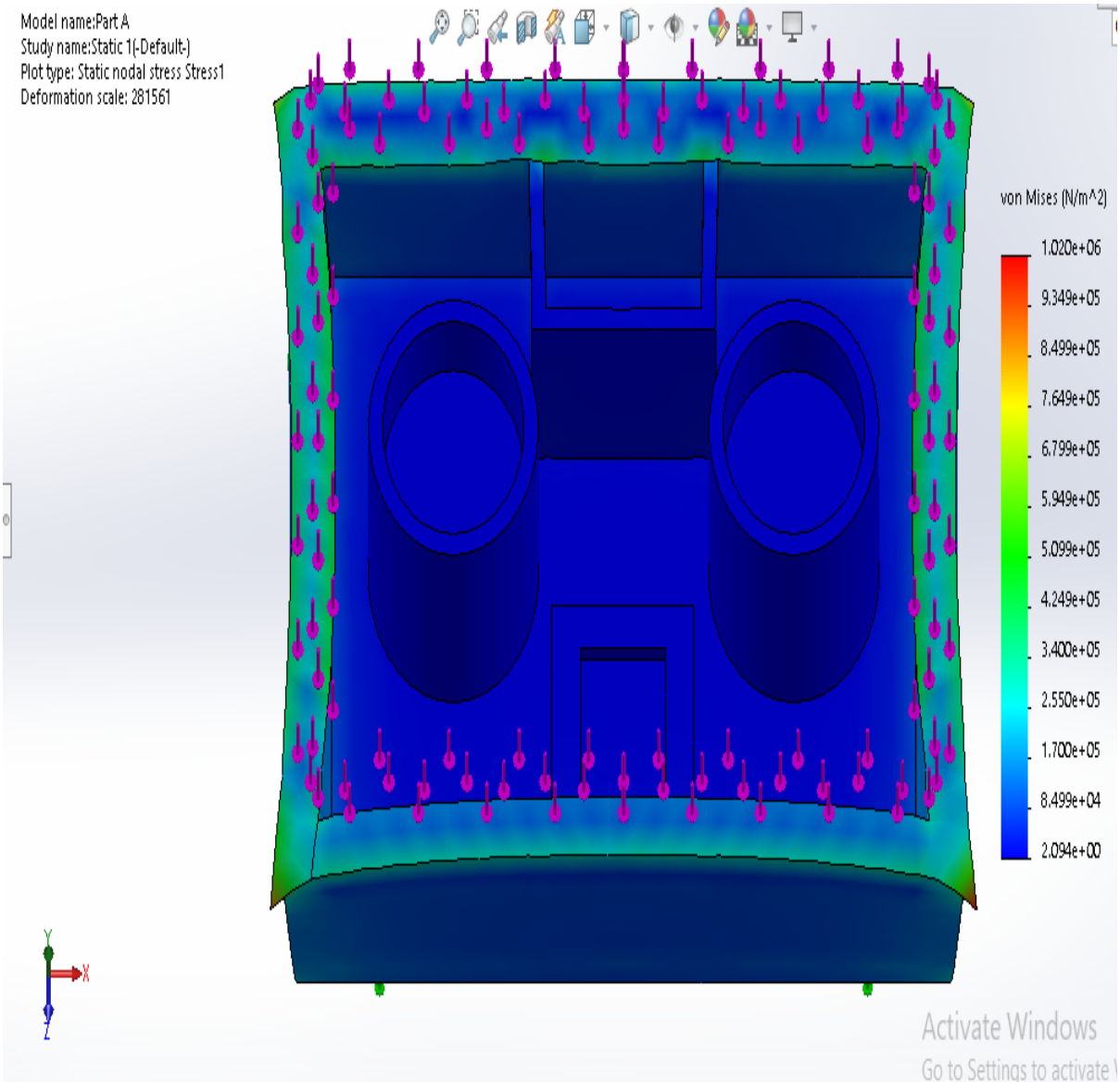
Model name:Part A
Study name:Static 1(-Default-)
Plot type: Static nodal stress Stress1
Deformation scale: 281561
von Mises (N/m^2)
1.020e+06
9.349e+05
8.499e+05
7.649e+05
6.799e+05
5.949e+05
5.099e+05
4.249e+05
3.400e+05
2.550e+05
1.700e+05
8.499e+04
2.094e+00
Activate Windows
Go to Settings to activate

Static Simulation of stresses of 1000N.

Appendix C

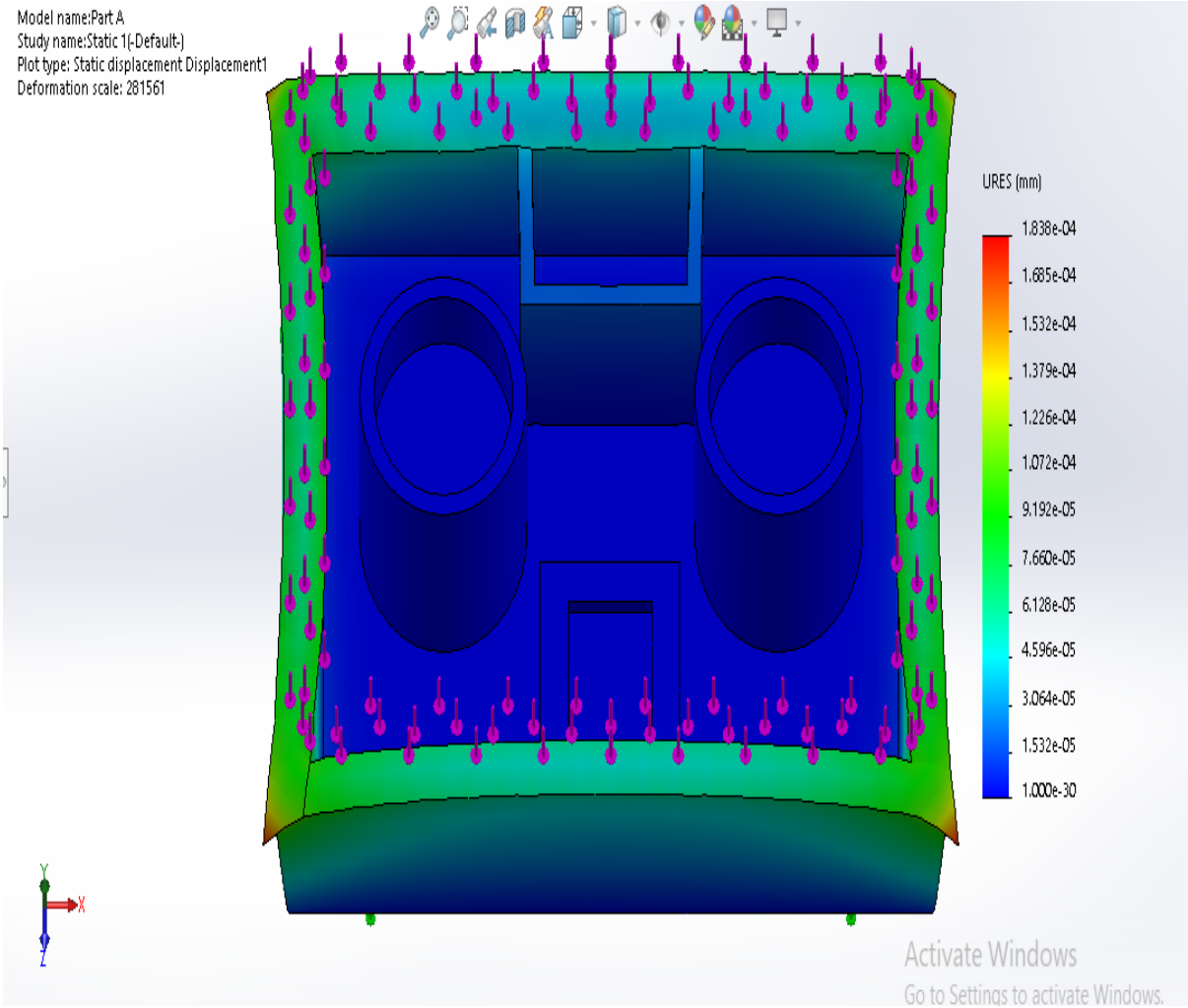

Static Simulation of displacement of 1000N.

Appendix D

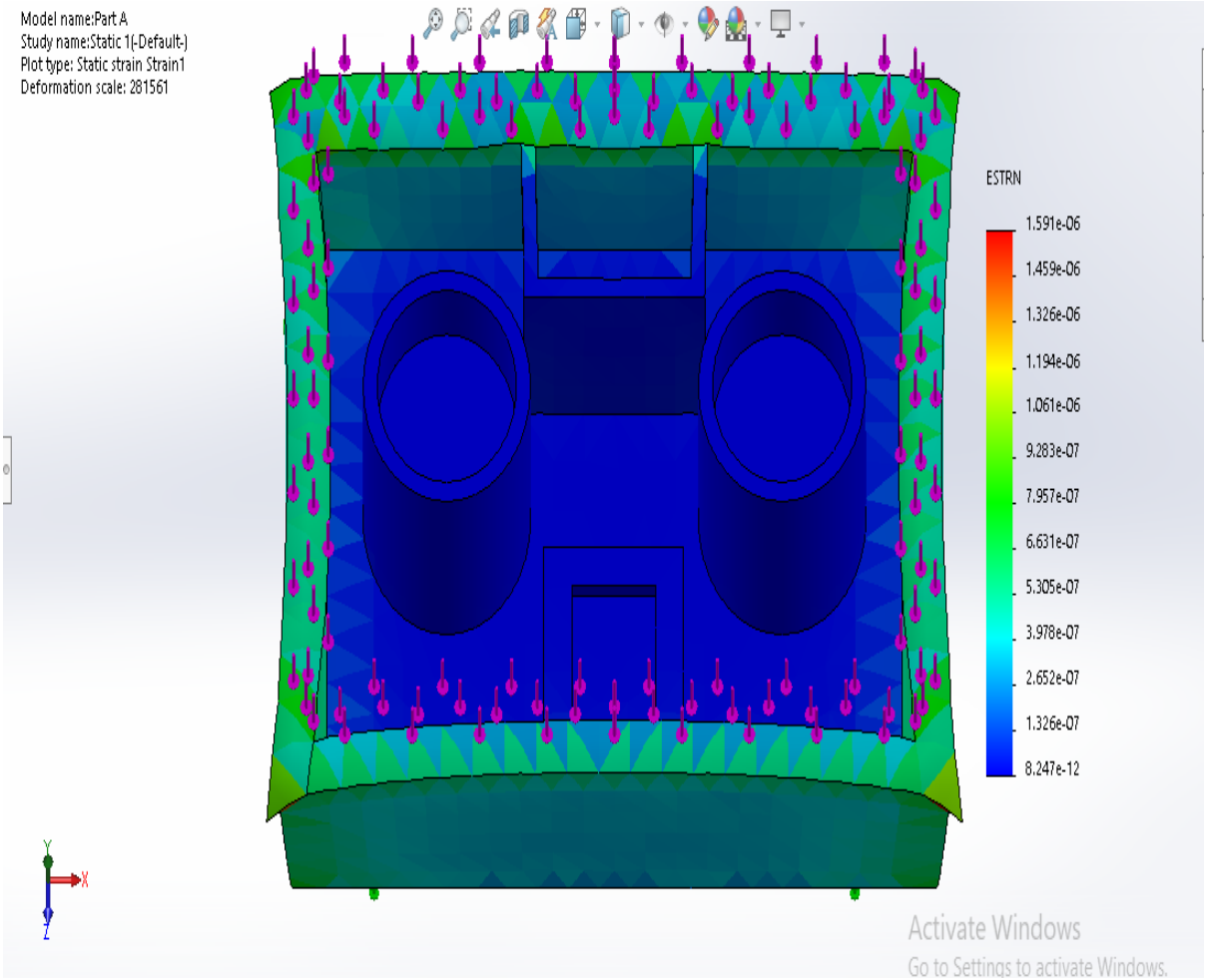

Static Simulation of the strain of 1000N.